



# Cryogenic transmission electron microscopy (cryo-TEM) for studying the morphology of colloidal drug delivery systems

Judith Kuntsche<sup>a</sup>, Jennifer C. Horst<sup>b</sup>, Heike Bunjes<sup>b,\*</sup>

<sup>a</sup> Martin-Luther-Universität Halle-Wittenberg, Institute of Pharmacy, Department of Pharmaceutical Technology and Biopharmaceutics, Wolfgang-Langenbeck-Str. 4, D-06120 Halle (Saale), Germany

<sup>b</sup> Technische Universität Braunschweig, Institute of Pharmaceutical Technology, Mendelssohnstr. 1, D-38106 Braunschweig, Germany

## ARTICLE INFO

### Article history:

Received 20 December 2010

Received in revised form 29 January 2011

Accepted 1 February 2011

Available online 16 February 2011

### Keywords:

Transmission electron microscopy

Cryoelectron microscopy

Colloidal drug carrier systems

Liposomes

Nanoparticles

Colloidal emulsions

## ABSTRACT

Cryogenic transmission electron microscopy (cryo-TEM) has evolved into an indispensable tool for the characterization of colloidal drug delivery systems. It can be applied to study the size, shape and internal structure of nanoparticulate carrier systems as well as the overall colloidal composition of the corresponding dispersions. This review gives a short overview over the instrumentation used in cryo-TEM experiments and over the sample preparation procedure. Selected examples of cryo-TEM studies on colloidal drug carrier systems, including liposomes, colloidal lipid emulsions, solid lipid nanoparticles, thermotropic and lyotropic liquid crystalline nanoparticles, polymer-based colloids and delivery systems for nucleic acids, are presented in order to illustrate the wealth of information that can be obtained by this technique.

© 2011 Elsevier B.V. All rights reserved.

## 1. Introduction

Colloids like nanoparticles, liposomes and micelles are intensively being studied for drug delivery purposes to improve the therapeutic efficiency by specific delivery of the drug to the site of its action using passive and/or active targeting strategies. Furthermore, incorporation into a carrier may protect the drug from degradation in biological fluids or may provide an applicable formulation of the drug for the desired route of administration, e.g. by solubilization of poorly water soluble substances (Allen and Cullis, 2004; Couvreur and Vauthier, 2006).

In addition to the general properties of colloidal formulations (e.g. composition, drug incorporation efficiency, particle size and size distribution), the morphology of the colloidal carriers is of utmost importance. Transmission electron microscopy (TEM (Friedrich et al., 2010)) is most frequently used for the evaluation of the ultrastructure of colloidal drug carrier systems next to scanning electron microscopic techniques (SEM, ESEM) and atomic force microscopy (AFM). The different methods of sample preparation for TEM (e.g. negative staining, freeze-fracture and vitrification by plunge freezing)

can provide different information about the colloidal structures.

Due to its speed and simplicity, negative staining (Friedrich et al., 2010; Harris, 1997, 2007) is the most commonly used preparation method for the evaluation of colloidal formulations by TEM. A drop of the sample is placed on a TEM grid (small round gold or copper grid with defined mesh size) and stained with a solution containing heavy metal salts which provide high contrast in the electron microscope (e.g. uranyl acetate). After drying, the sample is viewed in the electron microscope where the colloids (e.g. nanoparticles) appear bright against the darker background of the stain. Both staining and drying may result in structural alterations of the colloids which always need to be taken into consideration when interpreting negative staining TEM images. The freeze-fracture technique does not require a drying process and yields additional information about the internal structure of the nanoparticles (Kuntsche et al., 2004; Severs, 2007; Zasadzinski, 1986). The sample is dropped on a TEM grid which is then sandwiched between two copper or gold holders and vitrified by rapid freezing e.g. in liquid propane or melting nitrogen. Under constant cooling and in vacuum, the frozen sample is fractured with the fracture plane developing predominantly along areas of the sample with weak molecular interactions (e.g. within lipid bilayers). The fracture plane can further be etched (water sublimation in vacuum) and is shadowed with a thin platinum/carbon layer (about 2 nm) usually at an angle of 45° with respect to the fracture surface providing a “negative” replica of the fractured sample plane. Subsequently, a

\* Corresponding author. Tel.: +49 531 391 5657; fax: +49 531 391 8108.

E-mail addresses: [judith.kuntsche@pharmazie.uni-halle.de](mailto:judith.kuntsche@pharmazie.uni-halle.de) (J. Kuntsche), [jennifer.horst@tu-braunschweig.de](mailto:jennifer.horst@tu-braunschweig.de) (J.C. Horst), [heike.bunjes@tu-braunschweig.de](mailto:heike.bunjes@tu-braunschweig.de) (H. Bunjes).

thicker carbon layer (about 20–30 nm) is deposited onto the sample at an angle of 90° to improve the stability of the replica. After cleaning, usually with an organic solvent, to remove all organic residues, the replica is viewed in the electron microscope. As the platinum/carbon replicas are stable over time and upon TEM observation, they can be stored for later re-investigation. When obtained under optimal sample preparation conditions, freeze-fractured replicas reflect the original, native state of the sample. Artifacts may, however, easily occur, e.g. due to insufficient freezing rate or re-deposition of solvent molecules onto the sample plane after fracturing.

In contrast to the above mentioned methods, cryo-TEM after plunge freezing (Costello, 2006; Egelhaaf et al., 2000; Friedrich et al., 2010; Grassucci et al., 2007, 2008; Harris, 1997; Milne and Subramaniam, 2009; Unger, 2001) allows direct investigation of colloids in the vitrified, frozen-hydrated state, i.e. very close to their native state. As with freeze-fracture TEM, information about the internal structure of the colloidal particles may be obtained (e.g. for multilamellar vesicles, nanoparticles based on cubic or hexagonal phases). Cryo-TEM has particularly been used to analyze samples of biological origin like viruses, bacteria as well as thin cross sections of complex tissues (Jiang and Chiu, 2007; Marko and Hsieh, 2007; Norlén, 2007; Vanhecke et al., 2007). The fast developing techniques for all steps of sample preparation (e.g. environmental control during sample vitrification (Egelhaaf et al., 2000; Frederik and Hubert, 2005)) and data processing (e.g. digitalization of the data processing, CCD cameras (Unger, 2001)) resulted in wider use of this technique. Even information about the three-dimensional structure of the particles of interest (by three-dimensional reconstruction (Orlova et al., 1999) or cryoelectron tomography (Koning and Koster, 2009; Milne and Subramaniam, 2009)) is possible. Most organic materials give only a poor contrast in cryo-TEM but an improvement in contrast can be reached by combining staining techniques and cryo-TEM (Adrian et al., 1998; Wittemann et al., 2005). Another interesting cryo-TEM technique is the so-called freeze-fracture direct imaging, which is related to the freeze-fracture technique (Belkoura et al., 2004).

This review article aims at providing an overview about the possibilities of cryo-TEM analysis for pharmaceutical colloidal formulations. After a short introduction of the experimental setup for cryo-TEM as well as potential challenges and artifacts, selected cryo-TEM studies on various drug delivery systems are described. Due to the broadness of the field the goal is not an exhaustive review of the literature data. Instead, a selection of cryo-TEM studies on pharmaceutically relevant colloidal dispersions is presented in order to generate an impression of the possibilities and limitations of obtaining information on pharmaceutical systems by this experimental technique.

## 2. Experimental setup and sample preparation

### 2.1. The cryoelectron transmission microscope

The transmission electron microscope (TEM) (Williams and Carter, 1996) can be envisaged as an inverted light microscope in which the sample is, however, illuminated by an electron beam (Fig. 1A). At the top of the microscope column is the electron gun and a system of electromagnetic lenses focuses the electron beam on the sample. Transmitted electrons are projected onto a viewing screen or a photographic or electronic image recording device. As the electrons are easily deflected by, e.g. gas molecules, a high vacuum has to be maintained in the microscope column. Potentially evaporating material from the specimen (e.g. water molecules) is trapped by a decontaminator positioned close to the sample. Since electrons poorly

penetrate matter, only thin samples or sample sections can be studied.

The contrast in TEM is obtained by the interaction of the electrons with the material (scattering). Heavy metals like lead, uranium and platinum strongly interact with the electrons and are, therefore, often used to improve the contrast (e.g. negative staining with uranyl acetate). The resolution in the TEM is directly proportional to the acceleration voltage of the electrons: with increasing voltage the wavelength of the electrons decreases resulting in higher resolution. On the other hand, the contrast becomes poorer with increasing acceleration voltage as the scattering of the electrons is inversely proportional to their velocity. In TEM investigations on colloidal drug carrier systems voltages between 80 and 200 kV are usually applied.

In cryo-TEM, the sample is directly visualized in the frozen-hydrated state and some additional features to the conventional transmission electron microscope are required. The most important part of the cryo equipment is a specialized holder for the electron microscopic grid with the specimen (Fig. 1B). Typically, the holder contains a small dewar for liquid nitrogen as cooling agent at its end. Cooling of the tip of the holder is accomplished by a thermally conductive connection between dewar and tip (usually made of a copper alloy). The grid with the vitrified film is placed into this cooled tip and fixed, e.g. with clamp rings. A good mechanical and thus thermal contact between holder tip and grid is essential to ensure adequate cooling of the sample. If the cooling of the sample is inadequate, the vitrified sample will be damaged by a kind of freeze drying effect (cf. Section 2.3). The holder also contains a shutter or gliding shield to protect the sample from contamination by cubic ice during the transport from the preparation or transfer unit to the TEM. Most cryo holders have an external temperature monitoring system connected to a thermocouple in the holder to observe the temperature during the whole procedure. Many holders also allow tilting of the samples during observation thus providing information about the three-dimensional structure (cryoelectron tomography (Jiang and Chiu, 2007; Marko and Hsieh, 2007; Milne and Subramaniam, 2009)).

During the transport of the holder between sample preparation unit and TEM, an additional protection system is required for the tip of the holder to avoid ice formation on the shutter or holder as this may damage the shutter system by freezing and bring moisture into the vacuum of the TEM. Different protection systems are commercially available, e.g. bellow systems or gas shield devices in the form of a cartridge, which are flushed by a stream of dry nitrogen gas. Some laboratories use homemade systems, e.g. made of styrofoam. As introduction of water into the TEM is almost inevitable due to condensation on cold parts of the holder, a second decontaminator is often installed in the vacuum of the cryo-TEM, which is placed on both sides of the sample and cooled by liquid nitrogen. Decontaminators also remove water molecules evaporating from the sample during observation.

### 2.2. Sample preparation

Sample preparation for cryo-TEM is a rather sensitive process requiring strict control of sample environment over the whole time of preparation, transfer and electron microscopic investigation. Automated vitrification systems with controlled humidity (Fig. 1C; Egelhaaf et al., 2000; Frederik and Hubert, 2005) are recommended to ensure a reproducible sample preparation procedure. Specialized equipment often contains an environmental chamber that allows sample preparation at defined humidity and/or non-ambient temperatures.

For cryo-preparation, sample concentrations of about 1–2 mg/ml are recommended (Harris, 1997) but the optimal concentration may vary. The size of the particles in the sample

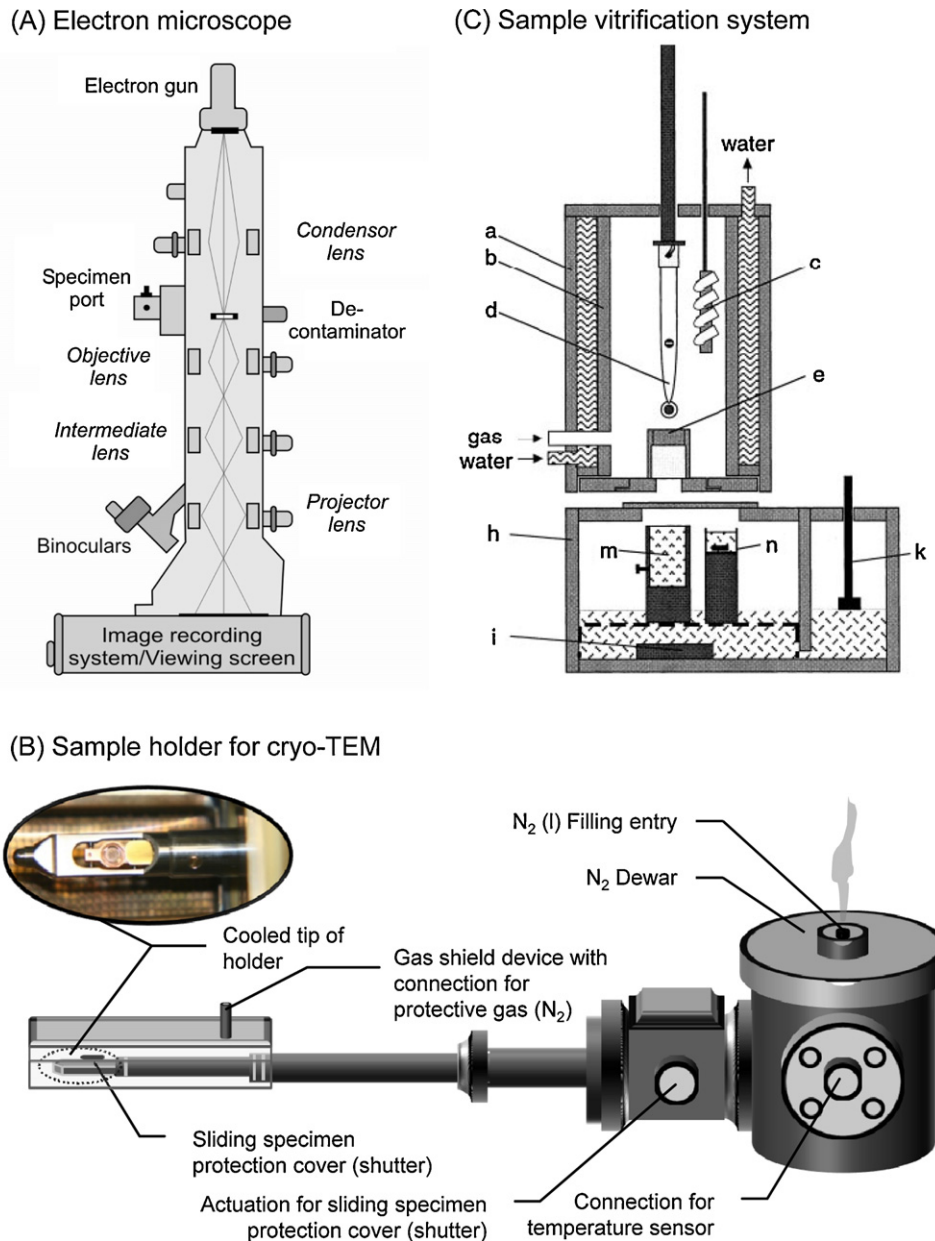


**Fig. 1.** (A) Schematic presentation of a transmission electron microscope and the electron path. (B) Sketch of a sample holder with integrated supplementary functions for use in cryo-TEM investigations. The photograph shows the tip of an Oxford CT-3500 cryo holder for a Zeiss Leo 922 Omega TEM with open shutter and inserted grid. (C) Automated sample vitrification system for cryo-TEM according to Egelhaaf et al. (2000). The chart shows schematically a cross section of the environmental chamber with the sample grid fixed with tweezers (d), the acrylic glass blocks (e) over which filter paper can be stretched for blotting excess sample, and a polystyrene box (freezing chamber) containing liquid nitrogen (h) with two vessels (m, n). The temperature in the upper part of the freezing chamber is held at  $-170^{\circ}\text{C}$ . The sample is plunged into the vessel filled with cryogen (m) which is shown in its upper position but can be lowered after plunging to allow removal of the vitrified specimen from the cryogen and the latter to drain off. The whole polystyrene box is then shifted and the sample is positioned in the second vessel (n) filled with liquid nitrogen and containing the transfer box. Further annotations: a and b: acrylic glass tubes forming the double wall of the chamber; c: holder for sample equilibration; i: resistor for gentle heating of liquid nitrogen to produce a flow of nitrogen gas; k: polystyrene floater with wooden slat to indicate nitrogen level. Panel C reprinted and modified with permission from Egelhaaf et al. (2000).

should be in the lower nanometer range since large particles are likely to be removed from the sample film during blotting. In order to allow for a reasonable blotting procedure and to span an acceptable film, the sample must not be too viscous. As a rule of thumb, an aqueous sample is suitable for the cryo-preparation technique if a drop of sample spreads comparably to water on a filter paper.

Although bare grids, e.g. made from copper, are also in use, carbon coated holey grids are usually more convenient and most commonly used in cryo-TEM studies. Carbon coated holey grids have a squared copper mesh which is covered with a carbon coated foil perforated by holes that can have different shapes (e.g. circu-

lar, hexagonal, square or orthogonal). For carbon coated grids, a glow discharge is performed directly before sample application in order to hydrophilize the grid for optimal spreading of the aqueous sample.

After fixation of the TEM grid in the preparation chamber, a droplet of sample (approximately  $2\text{--}5\ \mu\text{l}$ ) is applied to the grid with a pipette. Excess of sample is removed by quick blotting with a filter paper leaving a thin spanned film of the sample in the holes of the grid and the sample is then immediately plunge frozen in liquid ethane. A very high cooling rate is required to vitrify the sample (i.e. transform it into a glassy state) and to avoid the formation of crystalline (cubic or hexagonal) ice (Roos and Morgan, 1990).

Liquefied ethane cooled to liquid nitrogen temperature is a common cryogen for vitrification of cryo-TEM samples. Evaporation effects before freezing must strictly be avoided by preparation of the sample in a chamber with controlled humidity as mentioned above or by providing wet filter paper close to the sample. After freezing, the sample needs to be kept at very low temperatures (e.g. around  $-175^{\circ}\text{C}$ ) in order to avoid phase transition of the vitrified water into crystalline ice. Under cooling, the grid with the vitrified sample is removed from the container with liquid ethane and excess ethane is blotted with a piece of filter paper. The sample is transferred intermediately into liquid nitrogen and inserted into the cold cryo holder using pre-cooled tools. Subsequently, the cooled holder is quickly transferred to and inserted into the electron microscope. Care needs to be taken to avoid contact with atmospheric moisture which can lead to a contamination with cubic ice on cooled parts of the cryo holder, the vitrified specimen or the transfer unit.

Altogether, sample vitrification, insertion of the sample into the holder and transfer of the holder into the TEM should only take a few minutes to avoid contamination with cubic ice or variations in temperature.

### 2.3. Investigation of the sample and potential artifacts

Cooling needs to be continued after insertion of the holder into the electron microscope since inadequate cooling will result in damage of the vitrified sample by a kind of freeze drying effect in the vacuum of the TEM (Fig. 2A). The colloidal structures embedded into the thin film are viewed under low dose conditions to avoid electron beam damage. The sample is first viewed in an overview mode (Fig. 2B) and the positions of the most promising parts of the sample film can be saved. After switching to the magnification for sample imaging, an aperture system should be activated to limit the illumination to the viewed area thus protecting other sample areas from electron beam damage. As many cryo-TEM samples generally have a low contrast, an aperture system and an energy filter can be used to amplify the contrast and a slight underfocus is mostly adjusted, which appears as enhanced contrast to the eye (Scherzer defocus). In addition, a variation in focus can help to distinctly show different parts of a structure, while a total defocus creates optical artifacts. Images are usually taken by digital camera systems with an image-processing software. The images are processed by a computer program, which can subsequently enhance the contrast by several filter techniques. The time period of sample viewing in cryo-TEM is often limited as most samples are sensitive to radiation damages, frequently observed as “bubbling” of the structures (Fig. 2C).

As in other electron microscopic techniques, various artifacts may occur in cryo-TEM. For example, cryogen residues can remain from the plunge freezing process (Fig. 2D). Sometimes, these residues can be removed by carefully increasing the energy input. Warming of the sample by energy input may, however, lead to a phase transition of the vitrified ice into cubic or hexagonal ice (Fig. 2E). Ice contamination can also occur by a too high content of evaporated water in the column of the TEM (Friedrich et al., 2010). Since the sample film gets thinner in the middle of a hole of the grid, smaller particles are usually found in the middle part of the film. Larger particles, on the other hand, are often found near the division bars (Fig. 2F). In addition, anisometric particles like platelets may preferentially orientate parallel to the film surface (cf. section 3.3). Particles on division bars should not be interpreted because the film is not intact in these areas and embedded structures may be deformed.

It should always be borne in mind that TEM images only visualize a small part of the whole (more or less complex) sample. A

single TEM image should therefore not be overestimated and care should be taken to obtain a series of images that are representative for the whole sample.

## 3. Selected colloidal drug carrier systems studied by cryogenic transmission electron microscopy

### 3.1. Liposomes

Liposomes are vesicles composed of phospholipid bilayers encapsulating an aqueous inner compartment. In dependence on the size and the number of the phospholipid lamellae, liposomes can be classified into large or small unilamellar (LUV/SUV), multilamellar (MLV), oligolamellar (OLV) and multivesicular (MVV) vesicles. Liposomes are attractive membrane models to study, e.g. transport processes but also promising drug delivery systems as they can carry both hydrophilic (enclosed in the inner aqueous core), amphiphilic as well as lipophilic (located in the phospholipid bilayer) drugs. Cryo-TEM is a valuable tool to investigate, for example, the size, shape and lamellarity of liposomes and, consequently, liposome formulations have been studied intensively with this method (Almgren et al., 2000; Frederik and Hubert, 2005).

Due to the comparatively high contrast of the phospholipid bilayer, liposomes appear as characteristic ring-shaped structures in cryo-TEM images (Fig. 3). Preparation methods like extrusion or high-pressure homogenization result in formulations of mainly unilamellar vesicles but a more or less pronounced fraction of bi- or oligolamellar vesicles is usually also observed (see, e.g. Changsan et al., 2009; Dos Santos et al., 2002; Kaiser et al., 2003; Semple et al., 2005; Zhigaltsev et al., 2006). Holzer et al. (2009) used detergent removal – starting with a micellar solution of the phospholipid and detergent followed by subsequent dialysis to remove the detergent – and size exclusion chromatography (SEC) to produce essentially unilamellar vesicles with narrow size distribution (Fig. 3A). The rigidity of the lipid bilayer may influence the liposome shape: liposomes with a rigid lipid bilayer in the gel state often appear somewhat angular particularly when the vesicles are small in size (Fig. 3B) (Chiu et al., 2005; Kaiser et al., 2003; Kuntsche et al., 2010a). On the other hand, vesicle deformation and bilayer invaginations may occur when the lipid bilayer is highly flexible as, for example, in vesicles composed of soybean lecithin, ethanol and a terpene mixture (invasomes, Fig. 3C) (Dragicevic-Curic et al., 2008). Liposomes are rather fragile structures and processes like freezing and drying may result in morphological changes accompanied by a rearrangement of the vesicles (Changsan et al., 2009; Kim et al., 2007; Kuntsche et al., 2010a; Wessman et al., 2010) which is an important issue to consider particularly when hydrophilic drugs are encapsulated. The osmotic imbalance between the liposome core and the outer aqueous phase occurring during freezing and dehydration appears to be the main cause of the partial destabilization and rearrangement of the liposomes (Wessman et al., 2010).

Modification of the liposome surface to prolong the circulation time in the bloodstream can be realized by the addition of PEGylated phospholipids: DSPE-mPEG 2000 (1,2-distearoyl-sn-glycero-3-phosphatidylethanolamine-[methoxy(polyethyleneglycol)-2000]), for example, is frequently used for this purpose. However, DSPE-mPEG is a micelle-forming substance and in dependence on its concentration, disc-like mixed micelles may co-exist with vesicles until, at high concentrations of the PEGylated phospholipid, the vesicles disappear and mixed micelles of globular shape are formed (Edwards et al., 1997; Johnsson and Edwards, 2003). In cryo-TEM, the disc-shaped mixed micelles can clearly be distinguished from the vesicles and appear as small rods with high contrast (viewed edge on) or as circular structures with low uniform contrast (viewed face on, Fig. 3E and F). The size and shape of



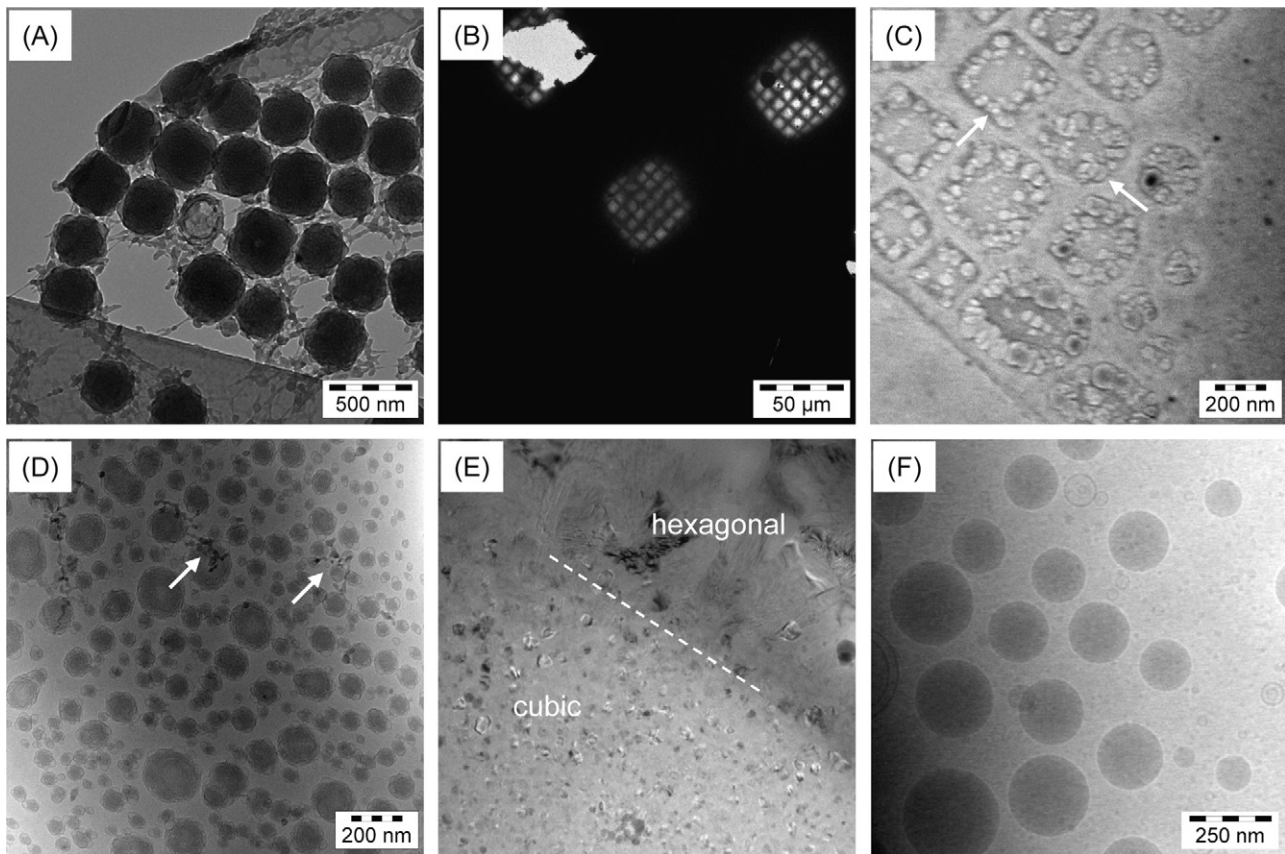


**Fig. 2.** Examples for artifacts that may occur in cryo-TEM illustrated on dispersions of cubic phase nanoparticles and the colloidal fat emulsion Lipofundin® MCT 20%. (A) “Freeze-drying-effect” in a film of cubic nanoparticles because of poor thermal contact between the grid with the vitrified sample film and the cooled holder tip. (B) Thick, but intact vitrified film (lower square) and partly damaged and ice-contaminated vitrified film (upper squares) on a Quantifoil holey carbon grid in overview mode. (C) Severe electron beam damage (“bubbling”) at the rims of cubic nanoparticles; the sample is continuously being damaged and therefore out of focus. (D) Ethane residues (arrows) from the vitrifying procedure on a film of cubic nanoparticles. (E) Hexagonal and cubic ice structures as a result of energy input by the electron beam. (F) Segregation of particles (emulsion droplets and liposomes) in a film of the emulsion Lipofundin® MCT 20: smaller particles remain in the thinner (brighter) parts of the film (middle of the hole) while larger particles can be found in thicker (darker) areas of the film close to the supporting bars (close to the lower left corner of the image). For more examples of artifacts see Friedrich et al. (2010) and Harris (2007).

the micelle discs as well as their frequency may vary in dependence on composition, way of preparation, thermal pre-treatment and storage conditions (Ickenstein et al., 2006; Sandström et al., 2008). Phospholipid hydrolysis has been found to enhance disc formation (Ickenstein et al., 2006). However, liposomes in the gel state (e.g. DPPC/DSPE-mPEG liposomes) may retain their vesicular structure even in the presence of hydrolysis products (Fig. 3D) as long as they are not heated above their phase transition temperature, which results in a more or less pronounced vesicle disintegration and rearrangement into disc-like micelles in dependence on the degree of hydrolysis (Fig. 3E and F) (Ickenstein et al., 2006). PEG-chains on the surface of liposomes are not visible in cryo-TEM images due to the low contrast of polyethylene glycol. In contrast, the polyelectrolyte shell of liposomes coated with positively charged poly(lysine) and negatively charged poly(glutamic acid) by the layer-by-layer technology could clearly be visualized by cryo-TEM (Ciobanu et al., 2007).

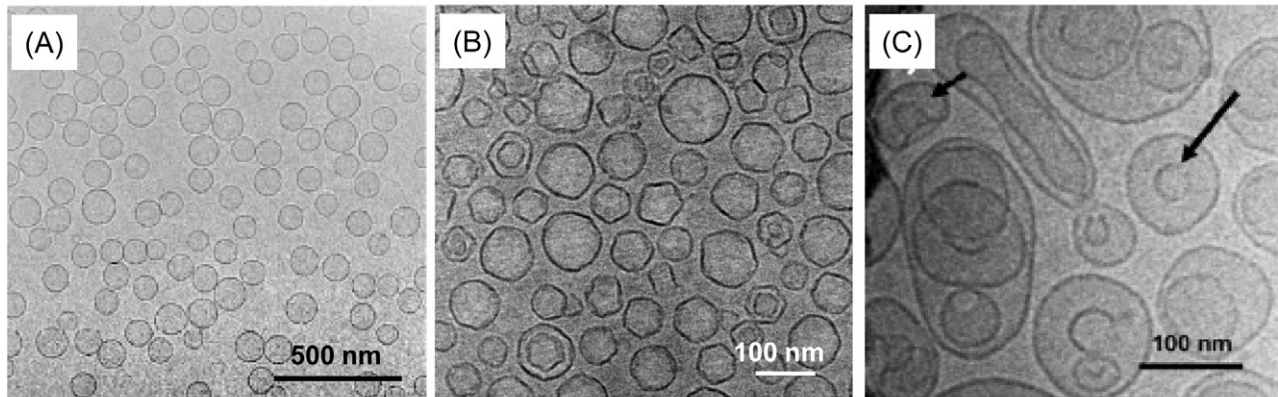
To improve the encapsulation efficiency for hydrophilic drugs and to reduce their leakage, the drugs can be loaded into and precipitated within liposomes by using pH- and/or ion-gradients over the liposome membrane. Drug precipitation could be visualized by cryo-TEM for various drugs encapsulated into liposomes, for example doxorubicin (Abraham et al., 2002; Chiu et al., 2005; Fritze et al., 2006; Li et al., 1998), idarubicin (Dos Santos et al., 2002), topotecan (Abraham et al., 2004; Taggar et al., 2006), vinorelbine (Semple et al., 2005; Zhigaltsev et al., 2006) and vincristin (Johnston

et al., 2006). Drug precipitates may appear as discrete structures in the liposome core (see e.g. the characteristic doxorubicin–citrate complexes in Li et al., 1998) or by an increase in contrast of the liposome core when the drug precipitates in amorphous form (Semple et al., 2005). Fondell and co-workers developed liposomes loaded with a radionuclide-labelled DNA binding compound (a  $^{125}\text{I}$ -labelled amino-benzyl derivative of daunorubicin) for tumor-cell specific nuclear therapy (nuclisome) (Fondell et al., 2010). Different aggregate structures were observed by cryo-TEM for the iodinated compound (spherical precipitates) and the non-iodinated one and doxorubicin, the latter two forming rod-shaped precipitates (Fig. 3G–I) (Fondell et al., 2010).

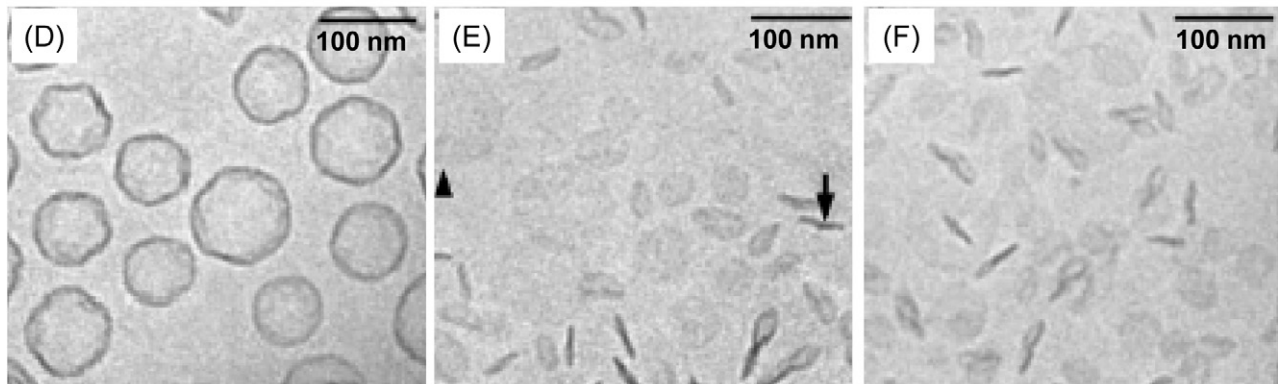
### 3.2. Colloidal fat emulsions

Colloidal fat emulsions have been in clinical use for parenteral nutrition for decades. Usually, they are composed of triglyceride oils (e.g. soybean oil, medium chain triglycerides [MCT]) and purified egg yolk lecithin as emulsifier. In cryo-TEM, the emulsion droplets appear as circular structures with an even distribution of contrast (Fig. 4) (Kuntsche et al., 2009; Rotenberg et al., 1991). They can easily be distinguished from vesicular structures (i.e. liposomes) which are present in such emulsions due to the excess of lecithin (Fig. 4A and B). Both, emulsion droplets and vesicles are usually rather heterogeneous in size. The vesicles are mostly unilamellar (Rotenberg et al., 1991) but bi- and even mul-

## Influence of bilayer composition



## Vesicle-micelle transformation



## Influence of drug loading

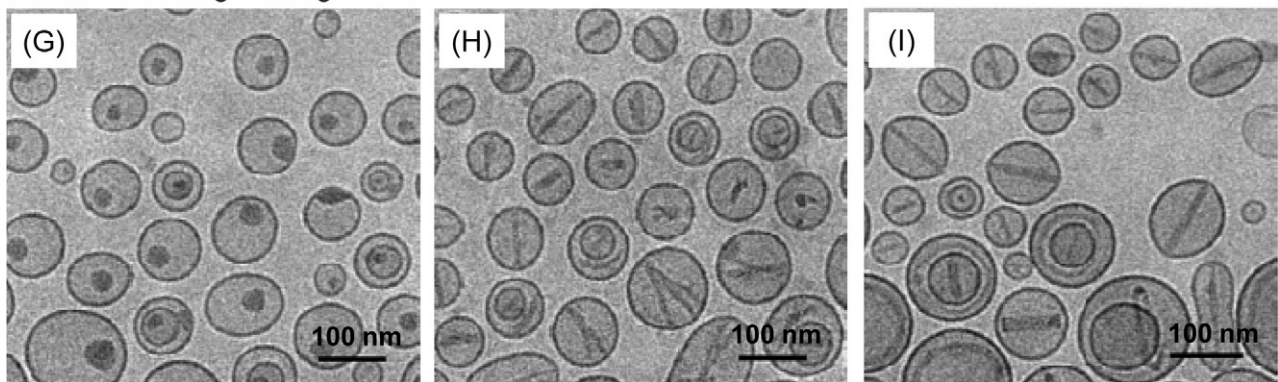


**Fig. 3.** Cryo-TEM images of different liposome formulations: (A) egg-yolk lecithin liposomes prepared by detergent removal and separated by size exclusion chromatography (SEC, sample obtained after retention time of 82 min) (Holzer et al., 2009); (B) liposomes composed of DSPC/DSPG (9:1 w/w) prepared by extrusion in 5% glucose solution (Kuntsche et al., 2010a); (C) invasive dispersion composed of 10% soybean lecithin, 3.3% ethanol and 1% of a terpene mixture (all concentrations w/v) (Dragicevic-Curic et al., 2008); (D–F) PEGylated liposomes (DPPC/DSPE-mPEG<sub>2000</sub>, molar ratio 90:4) prepared in citrate buffer pH 4 where the phospholipids are prone to hydrolysis, stored at 22 °C for 10 days and viewed in the cryo-TEM before (D) and after heating above the phase transition of the phospholipid (E). Note the presence of intact vesicles in (D) but their disintegration after thermal treatment (E). Liposomes stored at 4 °C for 67 days and viewed after heating above the phase transition temperature of the phospholipid (F). Cryo-TEM images of DSPC/cholesterol/DSPE-mPEG2000 liposomes (molar ratio 57:40:3) loaded with an iodinated amino-benzyl derivative of doxorubicin (G), the non-iodinated compound (H) and with doxorubicin (I). Abbreviations: DPPC – dipalmitoylphosphatidylcholine, DSPC – distearoylphosphatidylcholine, DSPG – distearoylphosphatidylglycerol. Reprinted from Holzer et al. (2009) (A), Kuntsche et al. (2010a) (B), Dragicevic-Curic et al. (2008) (C), Ickenstein et al. (2006) (D–F), all with permission from Elsevier. Panels G–I reprinted with kind permission from Springer Science and Business Media: Fondell et al. (2010, Fig. 2).

tilamellar vesicles could also be detected in some preparations (Fig. 4A) (Kuntsche et al., 2009). Colloidal fat emulsions bear some similarities to physiological carriers for lipophilic compounds (chylomicrons and triglyceride-rich lipoproteins, VLDL, very low density lipoprotein (van Antwerpen et al., 1999)) and are, consequently, also intensively studied as carrier systems for lipophilic drugs. In order to prolong the circulation time in the bloodstream the droplet surface can be modified with polyethylene glycol (PEG) chains – either by the addition of PEGylated phospholipids

(Wheeler et al., 1994) or by using polymeric stabilizers such as PEG-containing block copolymers (de Vries et al., 2010; Jores et al., 2004). This does not alter the overall appearance of the emulsion droplets in the cryo-TEM images (de Vries et al., 2010; Jores et al., 2004) due to the above mentioned low contrast of polyethylene glycol. Nevertheless, modification of the emulsifier system may result in alterations of the morphology of the emulsion droplets (Teixeira et al., 2000) or in the formation of additional structures beside the emulsion droplets (Klang et al., 2010). Admixture of the positively



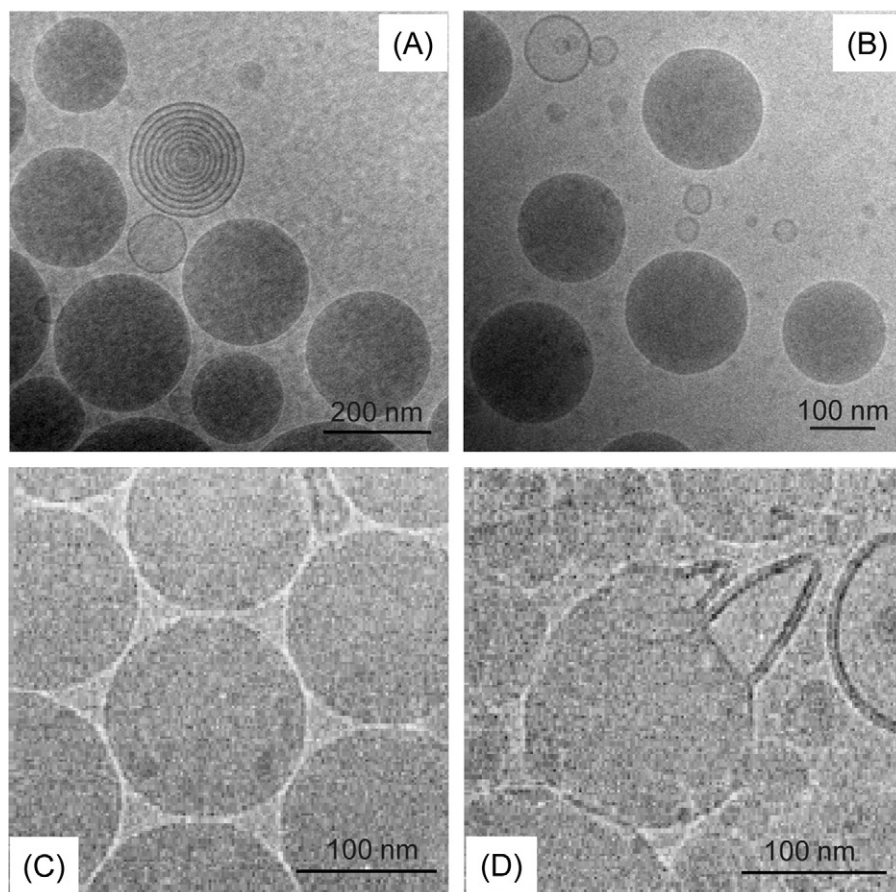


**Fig. 4.** Images of colloidal fat emulsions obtained by cryo-TEM: (A) Lipofundin® 20% N, (B) Lipofundin® MCT 20%, (C) and (D) triglyceride emulsions stabilized with egg yolk lecithin alone (C) and with the admixture of stearylamine for surface modification (D). Note the formation of “handbag”-like structures in the presence of stearylamine in the emulsions (D). (C and D) with kind permission from Springer Science and Business Media: Teixeira et al. (2000, Fig. 2a and c).

charged stearylamine to egg yolk lecithin for the stabilization of an MCT emulsion led to the formation of membrane extrusions of the stabilizer(s) at the interface of the emulsion droplets appearing as “handbag”-like structures in the cryo-TEM images (Fig. 4D) (Teixeira et al., 2000). It has been hypothesized that a partial phase separation of the lipidic emulsifier mixture at the interface may be responsible for the formation of these characteristic structures (Teixeira et al., 2000).

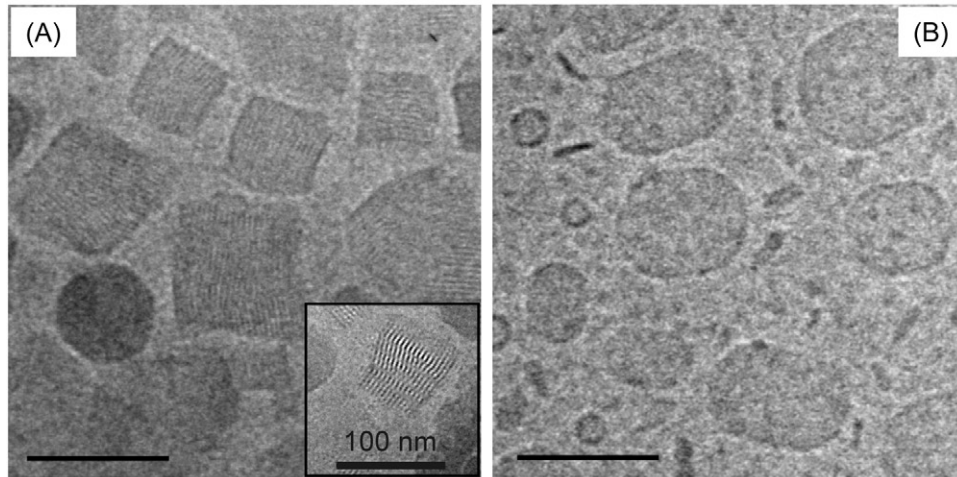
### 3.3. Solid lipid nanoparticles

Solid lipid nanoparticles (colloidal suspensions of crystalline lipids) are also intensively being studied as drug carrier systems. Cryo-TEM investigations were used to clarify some important structural features of these systems. For example, they confirmed the formation of very anisometric, platelet-shaped particles upon crystallization of spherical triglyceride nanodroplets after processing by melt-homogenization (Petersen et al., submitted for publication; Westesen and Siekmann, 1997; Westesen et al., 2001). Depending on the angle of observation in the vitrified sample, these particles may appear as circular, ellipsoidal or elongated edged structures (top-view on the platelets) or as needle-like structures of higher contrast (platelets viewed edge-on). Often, the platelet-like particles orientate preferentially with their large surface in parallel to the surface of the vitrified film and are thus imaged in top-view. The possibility to measure the thickness of single platelets in cryo-TEM images was utilized to support investigations on the particle size dependent melting behavior of triglyceride nanoparticles (Bunjes et al., 2000; Unruh et al., 1999). Different shapes

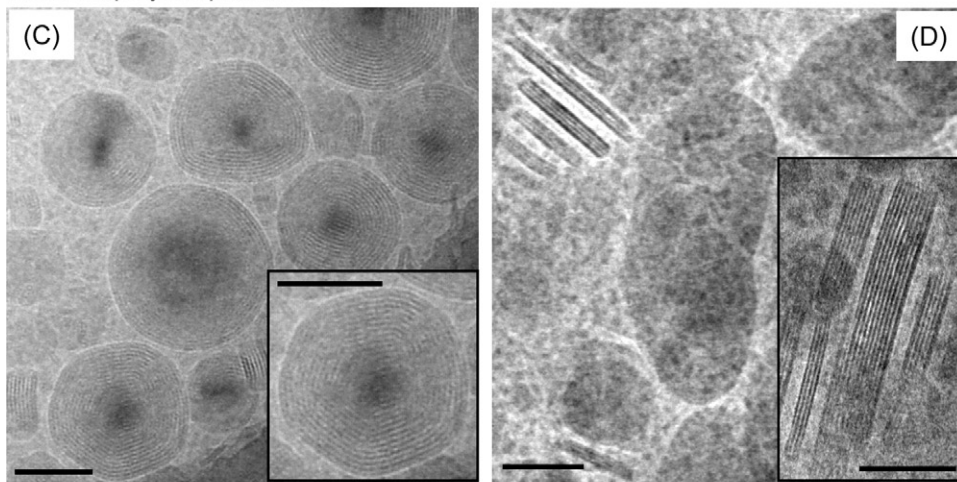
of the particles were observed in dependence on their composition and preparation process: triglyceride nanoparticles in the  $\beta$ -modification stabilized with polyvinyl alcohol (PVA), for example, appeared less anisometric and more block-like compared to the thin and extended platelets that are formed upon stabilization with a phospholipid-bile salt combination (Fig. 5A, B, D) (Petersen et al., submitted for publication; Rosenblatt and Bunjes, 2009). Also the shape of solid particles prepared from cholesteryl acetate by precipitation from solvent-in-water emulsions was found to be influenced by the type of emulsifier (Sjöström et al., 1995). Moreover, the shape of triglyceride nanoparticles can strongly depend on the polymorphic form of the matrix triglyceride as demonstrated for tristearin nanoparticles stabilized with PVA (Rosenblatt and Bunjes, 2009) or a phospholipid-bile salt mixture (Bunjes et al., 2007). In the metastable  $\alpha$ -modification, the particles were of spheroidal shape (Fig. 5C) whereas the  $\beta$ -form nanoparticles had the typical platelet-like shape and tended to self-organize in stacks (Fig. 5D). In this investigation, it could also be shown that it is possible to observe the organization of the lamellar triglyceride layers within single particles and to determine the polymorphic form of individual nanoparticles by the determination of the repeating unit of the lamellar layers (Bunjes et al., 2007). In cryo-TEM images of PVA stabilized trimyristin nanoparticles in the  $\beta$ -form, the nanoparticles did not only display the fine striations of the molecular layers but even step dislocations could be detected within some of the nanoparticles (Fig. 5A) (Rosenblatt and Bunjes, 2009).

Cryo-TEM played a major role in the elucidation of the ultrastructure of oil-loaded solid lipid nanoparticles, often called nanostructured lipid carriers (NLC). Compartments of liquid oil

## Influence of stabilizer



## Different polymorphic forms



## Loading with ubidecarenone

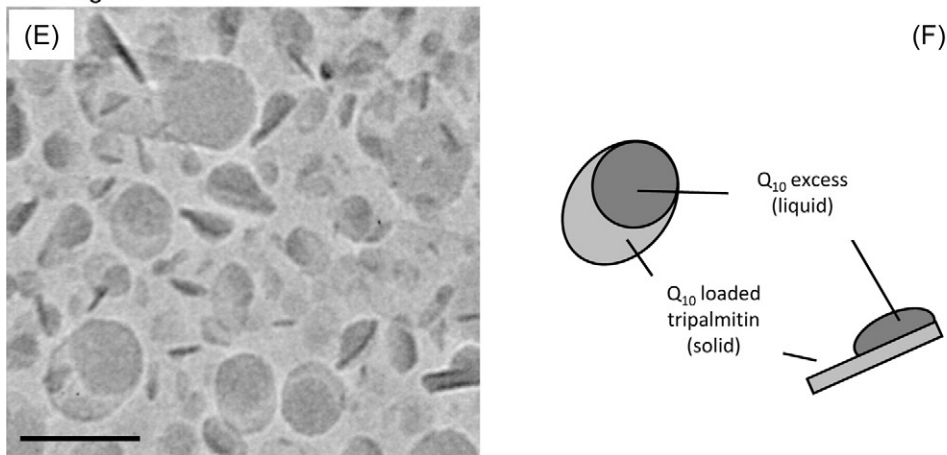


**Fig. 5.** Cryo-TEM images of solid lipid nanoparticles. (A and B) Morphology of trimyristin nanoparticles in the  $\beta$ -modification stabilized with poly(vinyl alcohol) (A) and with soybean lecithin/sodium glycocholate (B). The inset in (A) shows a filtered micrograph of a particle containing a step dislocation (Rosenblatt and Bunjes, 2009). Beside the crystalline nanoparticles phospholipid vesicles can clearly be detected as ring-like structures in (B) (data from Petersen et al., submitted for publication). (C and D) Morphology of tristearin nanoparticles stabilized with a mixture of saturated soybean lecithin (Lipoid S100-3) and sodium glycocholate. (C) Spheroidal particles in the  $\alpha$ -modification. (D) Platelet-shaped particles in the  $\beta$ -modification, which tend to pack in stacks at this concentration. The magnified particles shown in the insets display the internal striations reflecting the lamellar order of single molecular layers within the particles more clearly. Cryo-TEM micrograph (E) and schematic illustration (F) of tripalmitin nanoparticles loaded with 50% ubidecarenone ( $Q_{10}$ ). All scale bars represent 100 nm. Reprinted and adapted with permission from Rosenblatt and Bunjes (2009), American Chemical Society (A), Bunjes et al. (2007), American Chemical Society (C and D) and with kind permission from Springer Science and Business Media: Bunjes et al. (2001, Fig. 7b) (E and F).



sticking to the surface of the solid, platelet-like matrix of the nanoparticles were detected in several studies (Esposito et al., 2008; Jores et al., 2004). A similar appearance was also observed for triglyceride nanoparticles loaded with the low-melting lipophilic drug ubidecarenone (Fig. 5E and F) (Bunjes et al., 2001). In solid lipid nanoparticle dispersions containing phospholipids as stabilizers, phospholipid vesicles as additional colloidal structures have often been observed in the dispersions beside the triglyceride nanoplatelets (Petersen et al., submitted for publication; Sjöström et al., 1995; Westesen and Siekmann, 1997; Westesen et al., 2001) (Fig. 5B).

#### 3.4. Low density lipoprotein (LDL) and supercooled smectic lipid nanoparticles

Cholesterol esters are physiological lipids and occur in lipoproteins as storage and transport form of cholesterol. Cholesterol esters form thermotropic liquid crystalline phases (mesophases) and are the main component of the lipidic core of low density lipoprotein (LDL). LDL and LDL-like formulations appear promising also as carrier systems for lipophilic drugs particularly targeting cancer cells with high LDL receptor density (Firestone, 1994; Song et al., 2007).

At room temperature, LDL is in a liquid crystalline, smectic state and a cylindrical shape of the LDL was observed in cryo-TEM when sample preparation had been done at room temperature (Spin and Atkinson, 1995; van Antwerpen and Gilkey, 1994; van Antwerpen et al., 1997). By a computer-based analysis of the density profile of a large number of the anisometric particles imaged in different orientations, the three-dimensional structure of LDL could be reconstructed (Orlova et al., 1999). Interestingly, LDL does not display an even contrast in cryo-TEM. In side view, the top and the bottom of the cylindrical particles possess a higher contrast probably due to the attachment of apolipoprotein B with different electron density compared to the lipidic core of the LDL (Orlova et al., 1999; van Antwerpen and Gilkey, 1994).

The thermotropic mesomorphism of cholesterol esters together with the strong supercooling effect in the colloidal state has been explored for the development of dispersions of supercooled smectic lipid nanoparticles as drug delivery system for poorly water-soluble drugs (Kuntsche et al., 2004). Dispersions of smectic lipid nanoparticles usually appear rather heterogeneous in the electron microscope and both circular and angular structures can be observed (Fig. 6A–D) (Kuntsche et al., 2004, 2010b). Similarly as for LDL, a cylindrical shape of the smectic nanoparticles could be established by viewing the vitrified particles under different observation angles (Fig. 6E) (Kuntsche et al., 2010b). The smectic phase is a layered structure in which the cholesterol ester molecules are aligned side by side thus forming specific smectic layers (for details see (Kuntsche et al., 2004) and references therein). Cylindrical particles can easily accommodate the smectic layers whereas a spherical particle shape would result in a disturbance of the smectic structure in the core of the sphere. Cylindrical particles have different appearances in the cryo-TEM images depending on their orientation: rectangular in side view, circular in top view and oval-shaped in all intermediate (tilted) orientations (Fig. 6E). The emulsifier(s) have a strong influence on the particle shape which may vary from more or less closely cylindrical (when, for example, stabilized with phospholipids, Fig. 6A) to a more rounded oval shape (when stabilized, for example, with poloxamer, Fig. 6C). In phospholipid-containing dispersions, an additional particle fraction being highly unstable upon cryo-TEM observation was detected (Fig. 6B) (Kuntsche et al., 2004, 2005). Due to immediate “bubbling”, determination of the particle shape or morphology was not possible by cryo-TEM but images obtained by freeze-fracture TEM indicated the presence of spherical smectic lipid nanoparticles with concentric layers in addition to the majority of cylindrical ones (Kuntsche et al., 2005).

As already mentioned for colloidal fat emulsions and solid lipid nanoparticles (cf. Sections 3.2 and 3.3), other colloids formed by the excess of emulsifier(s) may co-exist with the smectic lipid nanoparticles when the stabilizer(s) tend to self-associate in aqueous media: vesicles, for example, are clearly visible in the cryo-TEM images of dispersions containing phospholipids (Fig. 6A) and the rough background in the image of the dispersion stabilized with polysorbate 80 may indicate the presence of small micelles (Fig. 6D).

#### 3.5. Dispersions of lyotropic liquid crystalline phases and related nanoparticles

In contrast to thermotropic mesophases, which form as a result of thermal treatment, lyotropic liquid crystalline phases (lyotropic mesophases) are ordered structures formed by amphiphilic molecules in contact with a solvent, e.g. with water. Prominent examples are the lyotropic cubic, hexagonal and lamellar phase. Certain lyotropic mesophases based on amphiphiles with comparatively low polarity (e.g. long-chain phospholipids or monoglycerides) which do not dissolve in contact with excess water can be dispersed into nanoparticles that retain the liquid crystalline structure. Since such particles contain both hydrophilic and lipophilic domains they are promising carrier systems for lipophilic, hydrophilic and amphiphilic drugs. The best-known example are liposomes (based on the lamellar mesophase) which are discussed in section 3.1. More recently, nanoparticles of lyotropic cubic, hexagonal and related structures (Fig. 7) have also been much investigated in the field of drug delivery. Cryo-TEM is an invaluable characterization method for such dispersions, as it allows visualizing the shape and the internal structure of the nanoparticles in detail.

The probably most intensely studied composition in this field consists of glycerol monooleate (GMO) dispersed in water with the polymeric surfactant poloxamer 407 (P407). The resulting nanoparticles are of reversed, bicontinuous cubic ( $V_2$ ) structure. With the help of cryo-TEM, important information on the influence of the P407/GMO ratio and the way of preparation on the internal structure and size range of such particles, e.g. the ratio between larger cubic particles and smaller vesicles (Fig. 7A–C), was obtained (Barauskas et al., 2005a; Gustafsson et al., 1997; Spicer et al., 2001; Wörle et al., 2006, 2007). By tilting the frozen-hydrated specimen in the electron microscope, Spicer et al. (2001) found some evidence that the outer shape of cubic nanoparticles may not necessarily be cube-like but more sphere-like or relatively flat. The cubic internal structure of GMO/P407 nanoparticles may be retained upon loading with drugs as, e.g. observed for indomethacin, dexamethasone or ubidecarenone (Efrat et al., 2009; Esposito et al., 2005; Gan et al., 2010). Generally, the structure of these particles is, however, quite sensitive towards alterations in composition. The addition of lipophilic compounds like triglyceride oils or vitamin A palmitate to the GMO/P407 system favors the formation of particles with hexagonal structure (Gustafsson et al., 1997) and also the formation of disordered structures as a result of drug loading has been reported (Efrat et al., 2009). The use of alternative dispersing agents can also lead to structural alterations in the dispersions (Murgia et al., 2010; Rangelov and Almgren, 2005). Almgren et al. (2007) demonstrated the usefulness of cryo-TEM investigations for the comparison of structures occurring in aqueous GMO dispersions stabilized with a hydrophobically modified ethyl hydroxyethyl cellulose ether over a broad range of different GMO/stabilizer/water ratios. They also followed the structural alterations of the dispersions over time and evaluated the influence of freeze drying on the structure of selected dispersions.

Since the use of monoglycerides as matrix material for liquid crystalline nanoparticles has raised some concern with regard

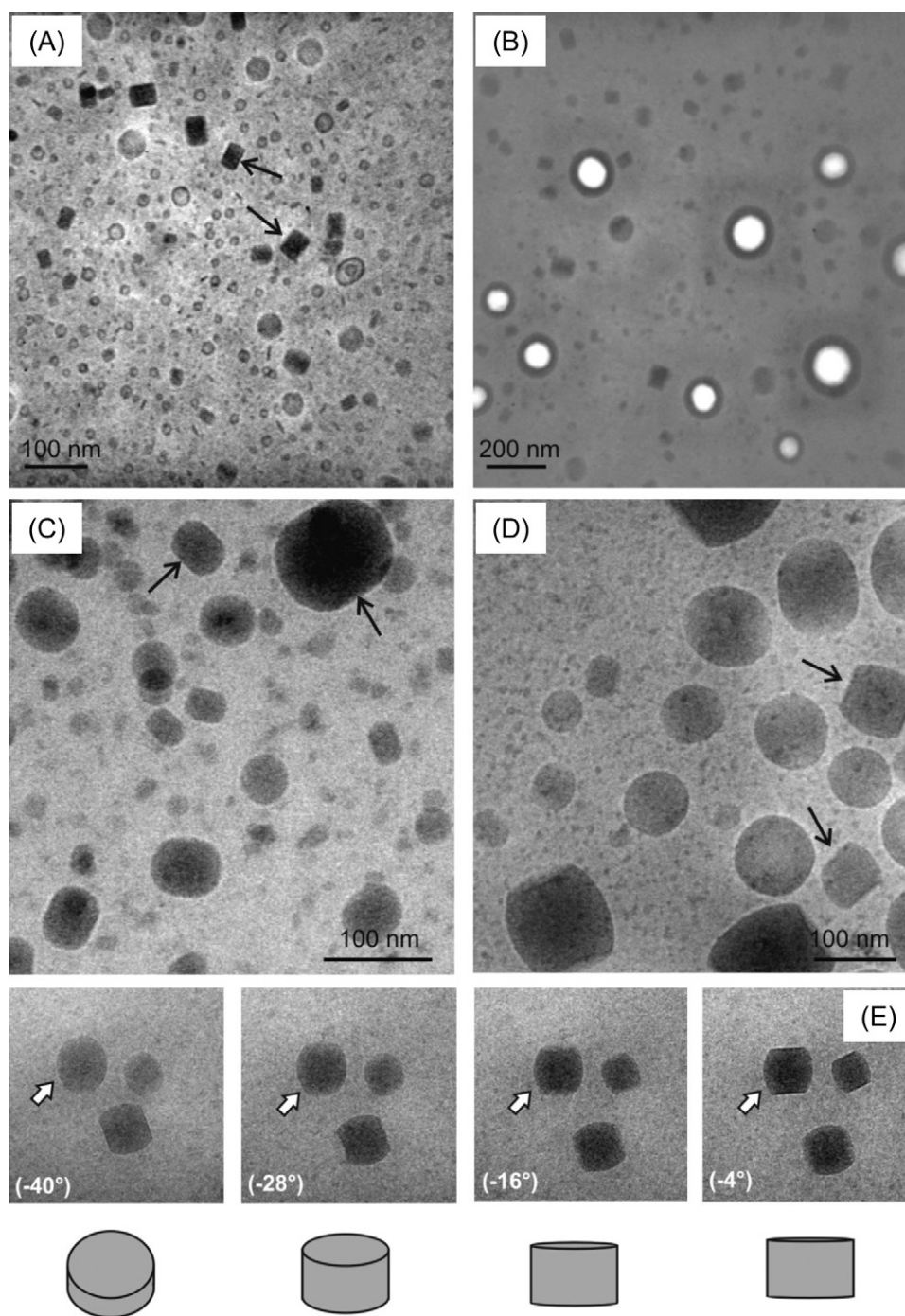


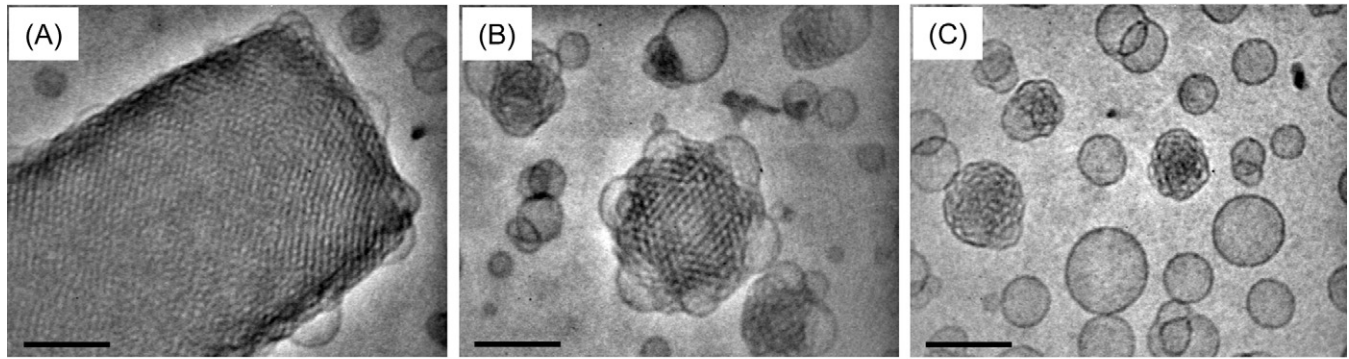
**Fig. 6.** Cryo-TEM images of dispersions of supercooled smectic cholesteryl myristate nanoparticles stabilized with soybean lecithin (Lipoid S100) and sodium glycocholate (A and B), poloxamer 188 (C) and polysorbate 80 (D and E). Some particles displayed in side-view are marked with arrows. The bright structures in (B) are “bubbling” nanoparticles leaving holes in the vitrified film (Kuntsche et al., 2005, 2010b). Cryo-TEM images of supercooled smectic nanoparticles taken at different angles of tilt (E). The appearance of the particles varies with their orientation as schematically illustrated below the micrographs for the particle marked with an arrow (Kuntsche et al., 2010b). Panels A and B reprinted from Kuntsche et al. (2005), panels C and E reprinted from Kuntsche et al. (2010b), all with permission from Elsevier.

to parenteral administration, several alternative compositions have been proposed, e.g. based on phospholipids. For example, the formation of particles with cubic internal structure was observed by cryo-TEM in dispersed mixtures of dioleoylphosphatidylethanolamine (DOPE) with PEGylated lipids (PEG-GMO or PEG-DOPE) (Johnsson and Edwards, 2001; Johnsson et al., 2005a). Particles consisting of a phosphatidylcholine/glycerol dioleate mixture stabilized with polysorbate 80 and loaded with propofol were already studied in vivo (Johnsson et al., 2006). In contrast to most other types of cubic particles, which are of bicon-

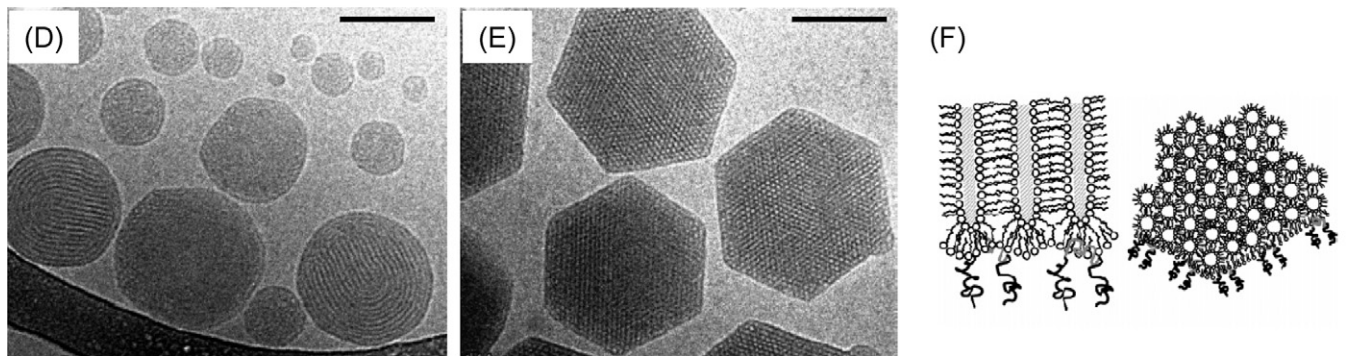
tinuous cubic ( $V_2$ ) structure, these particles contain a core of a reverse micellar cubic ( $I_2$ ) phase. Such particles were also observed in dispersions of a specific composition of the glycerol monolinoleate/tetradecane/P407/water system (Sagalowicz et al., 2007; Yagmur et al., 2006) (Fig. 8) whereas the corresponding tetradecane-free system formed particles of a bicontinuous cubic ( $V_2$ ) structure (de Campo et al., 2004; Yagmur et al., 2005). Tilt- ing experiments and fast Fourier transform (FFT) analysis of the cryo-electron micrographs can be of great help to unambiguously identify the different types of liquid crystalline structures (includ-



## Influence of composition on monoolein/poloxamer dispersions



## Influence of autoclaving on nanoparticles of hexagonal phase



## Influence of composition on “sponge” nanoparticles

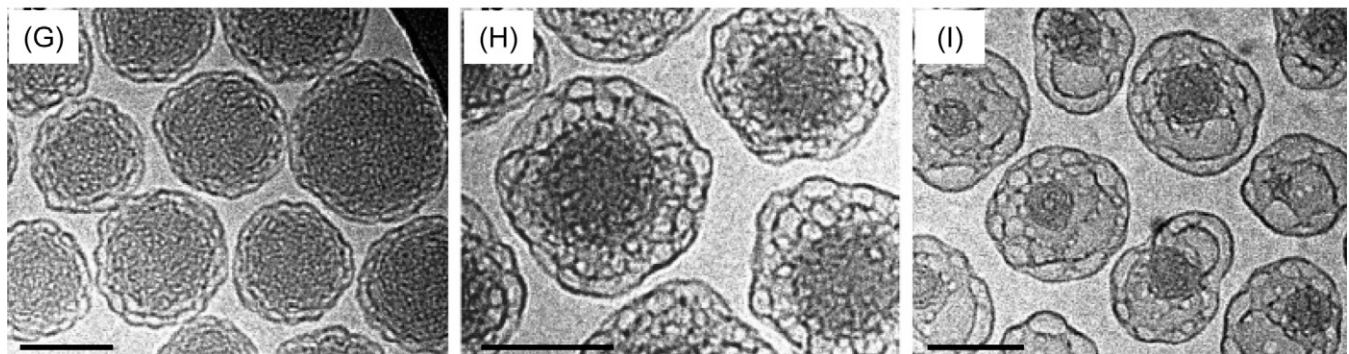


**Fig. 7.** Cryo-TEM micrographs of lyotropic liquid crystalline and related nanoparticles. (A–C) Monoolein/poloxamer 407 (P407) dispersions with increasing P407 concentrations in the monoolein/poloxamer mixture (A: 7.4%, B: 10%, C: 12% P407). (D–F) Nanoparticles of inverted hexagonal phase based on a diglycerol monooleate/glycerol dioleate 50/50 wt/wt lipid mixture that was dispersed with the help of poloxamer 407 (lipid/poloxamer 407 9/1 wt/wt) by shaking for 12 h at 350 rpm (D) and subsequently heat treated at 125 °C for 20 min (E). (F) schematically illustrates the structure of the inverse hexagonal phase leading to a striated appearance in side view and to a regular hexagonal pattern when viewed from the top of the particles. (G–I) “Sponge” nanoparticles based on a glyceroldioleate/diglycerolmonooleate 50/50 (wt/wt) lipid mixture dispersed with different amounts of polysorbate 80 (P80) by mechanical mixing (12 h at 350 rpm) in 95% water followed by heat treatment (125 °C, 20 min). Lipid/P80 90/10 (G), 80/20 (H), 70/30 (I). Scale bars represent 100 nm. (A–C) Reprinted from Wörle et al., 2007, with permission from Elsevier. (D–F) Reprinted with permission from Johnsson et al. (2005b), American Chemical Society. (G–I) Reprinted with permission from Barauskas et al. (2006), American Chemical Society.

ing the identification of the corresponding space groups) even on single particles as demonstrated by Sagalowicz et al. (2006, 2007) for glycerol monolinoleate-based dispersions (Fig. 8). Obtaining a series of suitable images may, however, be a major technical challenge due to the limited stability of the vitrified sample towards beam damage.

In addition to cubic phase nanoparticles, dispersions of hexagonal mesophases have intensively been studied. Such particles can, e.g. be obtained by adding nonpolar compounds such as triglyceride or alkane oil, to a monoglyceride-based particle matrix (Amar-Yuli et al., 2007; Gustafsson et al., 1997; Yagmur et al.,

2005). They were, however, also found in alternative compositions, e.g. in aqueous dispersions of glycerate surfactants or diglycerol monooleate/glycerol dioleate mixtures stabilized with P407 (Boyd et al., 2006; Johnsson et al., 2005b). Cryo-TEM investigations on diglycerol monooleate/glycerol dioleate/P407-based hexagonal nanoparticles revealed that the morphology of these particles strongly depended on the way of preparation. While rather round, striated particles were observed after simple mechanical dispersion, the particles transformed into well-shaped hexagons with a clear hexagonal internal pattern during an additional heat-treatment step (Fig. 7D–F). The results of tilting experi-



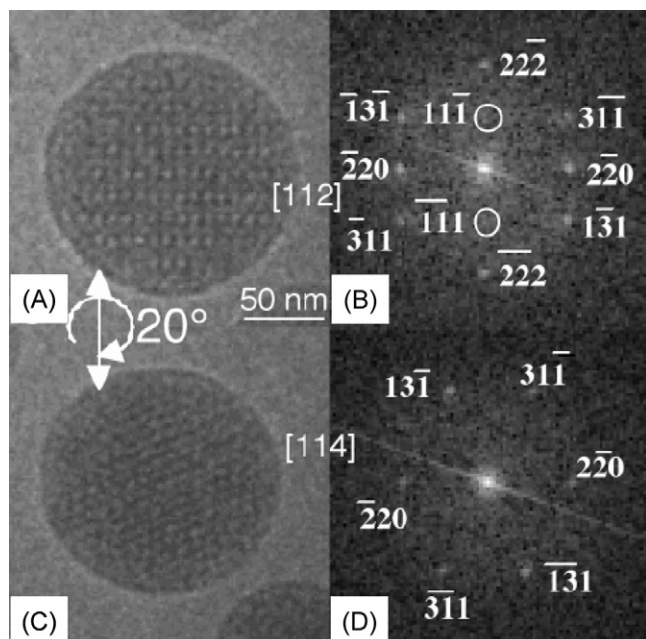


**Fig. 8.** Cryo-TEM images (A and C) of a nanoparticle with a micellar cubic structure ( $I_2$ , space group  $Fd\bar{3}m$ ) obtained under different angles of tilt (corresponding to the  $[112]$  and  $[114]$  axes of observation, respectively). Panels B and D show the fast Fourier transforms (FFT motifs) calculated from the images in A and C, respectively. The FFT motifs correspond to an optical diffractogram that reflects the structural symmetry, distances and angles contained in the respective cryo-TEM images. Dispersion composition: 3.3% monolinoleate, 1.3% tetradecane, 0.375% poloxamer 407, 95% water. Adapted with permission from Sagalowicz et al. (2007), American Chemical Society.

ments with these particles suggested a rather flat shape of the hexagons (Barauskas et al., 2005b). In contrast, cryo-field emission scanning electron microscopic investigations on hexagonally structured nanoparticles in a dispersion of phytantriol/vitamin E acetate/P407 indicated a more spinning-top-like shape of the hexagonal nanoparticles (Boyd et al., 2007).

Cryo-TEM investigations are an even more important characterization method for internally structured nanoparticles without a periodic internal pattern the structure of which cannot be elucidated in detail by other methods, such as, e.g. small angle X-ray diffraction. Such nanoparticles were, for example, observed in diglycerol monooleate/glycerol dioleate mixtures prepared with polysorbate 80 as dispersing agent (Barauskas et al., 2006). These particles, also termed “sponge” nanoparticles, are assumed to consist of a core of  $L_2$ -(reversed micellar) phase which is stabilized by a shell of  $L_3$ -(sponge) phase. The ratio of the two phases strongly depends on the lipid/polysorbate 80 mixing ratio (Fig. 7G–I). Glycerol monolinoleate/tetradecane-based nanoparticles containing a rather large fraction of tetradecane and dispersed with P407 also consist of an  $L_2$ -phase, however, without attached  $L_3$ -phase (Yagmur et al., 2005).

### 3.6. Polymer-based colloids

Amphiphilic block copolymers have widespread applications in the field of drug delivery. For this purpose, the hydrophilic block of the copolymers is usually composed of polyethylene glycol whereas a larger range of polymers is used to generate the hydrophobic part of the polymer. To improve the drug loading capacity – for example in polymeric micelles – as well as to prolong the release of the incorporated drug, the drug molecule may covalently be linked to the polymer (Hans et al., 2005).

Amphiphilic block copolymers may form various colloidal structures (spherical and worm-like micelles, vesicles) in dependence on the polymer architecture and the conditions during sample preparation. Spherical polymeric micelles appear as round structures with even contrast in cryo-TEM (Hans et al., 2005; Kim et al., 2008; Soga et al., 2005; Velluto et al., 2008). Polymeric vesicles (polymerosomes) may have different appearances in the cryo-TEM: they may be observed as characteristic ring-shape structures rather similar to liposomes (Discher et al., 1999; Ghoroghchian et al., 2006; Rank et al., 2009) or may possess a somewhat higher contrast also within the vesicle (del Barrio et al., 2010; Petrov et al., 2009; Yang et al., 2006; Yu et al., 2009).

The above mentioned colloidal structures shall be illustrated by a study of Rank and co-workers who used poly-2-vinylpyridine<sub>66</sub>-*b*-poly(ethylene oxide)<sub>46</sub> block copolymer (P2VP-PEO) for the preparation of vesicles in an aqueous medium (Rank et al., 2009). This polymer forms worm-like micelles at low temperature (predominant structures in Fig. 9A and B) but vesicles at room temperature (Fig. 9D). This behavior is due to an alteration of the molecular geometry in dependence on temperature with a cone-shaped geometry at 4 °C and a more cylindrical geometry at 25 °C. At 16 °C, intermediate structures (disc-like structures, open vesicles) co-exist with the worm-like micelles (Fig. 9B and C). Note also the presence of small spherical micelles (small dark dots) in Fig. 9A–C. Due to the thermotropic behavior of the polymer and re-arrangement into the final vesicles, very homogeneous vesicle dispersions could be prepared by controlled temperature treatment. By variation of the P2VP/PEO ratio, the final vesicle size could be adjusted (Rank et al., 2009).

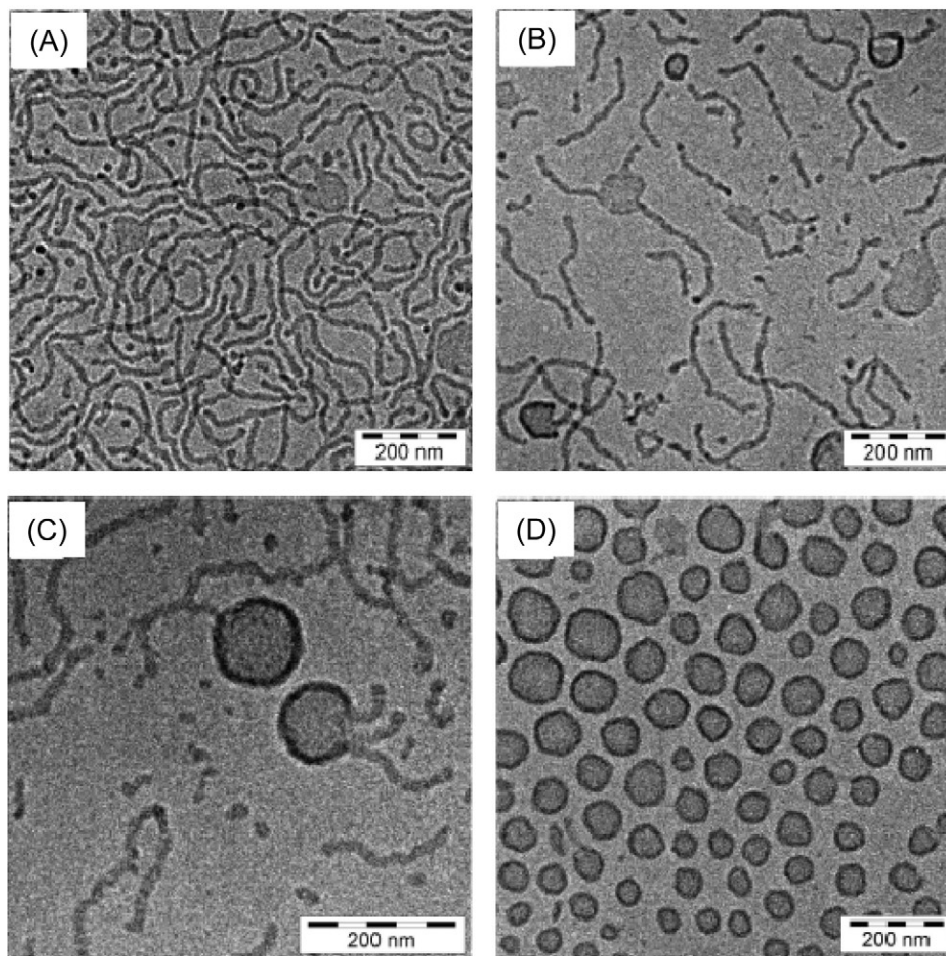
Wittemann et al. (2005) modified the surface of polystyrene nanoparticles with poly(styrene sulfonate acid) to prepare spherical polyelectrolyte brushes. The polyelectrolyte on the nanoparticle surface is difficult to detect by cryo-TEM due to its low contrast (Fig. 9E). However, replacement of the sodium counter-ions of the polyelectrolyte by caesium ions made the polyelectrolyte chains visible; an even better visualization was obtained after addition of bovine serum albumin which adsorbs to the polyelectrolyte and thus further increases the contrast (Fig. 9F). Even the collapse of the polyelectrolyte layer in the presence of high electrolyte concentrations could be visualized (Wittemann et al., 2005). Cryo-TEM was also used to study polystyrene nanoparticles modified with poly(*N*-isopropylacrylamide) to obtain thermo-sensitive core-shell particles. It was possible to follow the temperature dependent shrinkage of the thermo-sensitive nanoparticle shell and a good agreement between data obtained by dynamic light scattering, small angle X-ray scattering and cryo-TEM could be established (Crassous et al., 2006, 2009).

### 3.7. Delivery systems for nucleic acids

The administration of nucleic acids, e.g. in the form of whole plasmids, oligonucleotides (ODN) or small interfering RNA (siRNA) may open up a large range of important therapeutic possibilities. Unfortunately, these molecules possess very unfavorable biopharmaceutical properties since they are large, highly charged and sensitive towards enzymatic degradation. Thus, they need to be processed into suitable delivery systems, typically by interaction with cationic lipids, surfactants or polymers. The resulting complexes are usually of colloidal size and their structure has been intensively investigated by cryo-TEM. As the literature in this field is abundant, in particular concerning the structure of complexes with lipids (lipoplexes), only a few examples will be mentioned here. Some of the cryo-TEM work on lipoplexes was recently reviewed by Alfredsson (2005).

The complexation of large DNA molecules with vesicle forming cationic lipids usually leads to aggregated and/or multilamellar

## Influence of temperature on self-assembly of P2VP-PEO



## Influence of staining

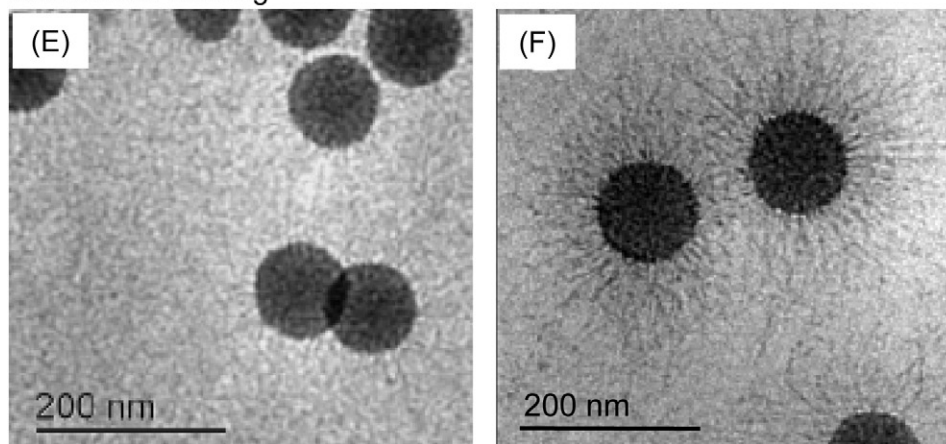


**Fig. 9.** Cryo-TEM images of a dispersion of poly-2-vinylpyridine<sub>66</sub>-b-poly(ethylene oxide)<sub>46</sub> block co-polymer (P2VP-PEO) micelles after storage at 4°C and subsequent warming to 16°C (A–C) and to 25°C (D). Images were taken after 1 h (A, D), 2.5 h (B) and after 24 h (C). Cryo-TEM images of a 1% suspension of spherical poly(styrene) nanoparticles grafted with long chain poly(styrene sulfonate acid) prepared by photoemulsion polymerization (E and F) at low salt concentration in the medium where the polyelectrolyte chains are strongly stretched. Compared to the original preparation (E) the contrast is enhanced by replacement of the sodium counterions by caesium ions and the addition of bovine serum albumin (F). Reprinted with permission from Rank et al. (2009), American Chemical Society (A–D) and with permission from Wittemann et al. (2005), American Chemical Society (E and F).

structures (Clement et al., 2005; Gustafsson et al., 1995; Huebner et al., 1999; Perrie et al., 2001; Rodríguez-Pulido et al., 2008; Thierry et al., 2009). Similar structures but with the detailed characteristics depending on the oligonucleotide/lipid ratios were observed upon complexation with oligonucleotides (Maurer et al., 2001;

Semple et al., 2001; Weisman et al., 2004) (Fig. 10A). For example, particles with discrete membranes, paired membranes and condensed lamellar phase particles were observed in the study by Weisman et al. (2004). Based on their cryo-TEM results, the authors proposed a mechanism for lipoplex formation. Multilamel-



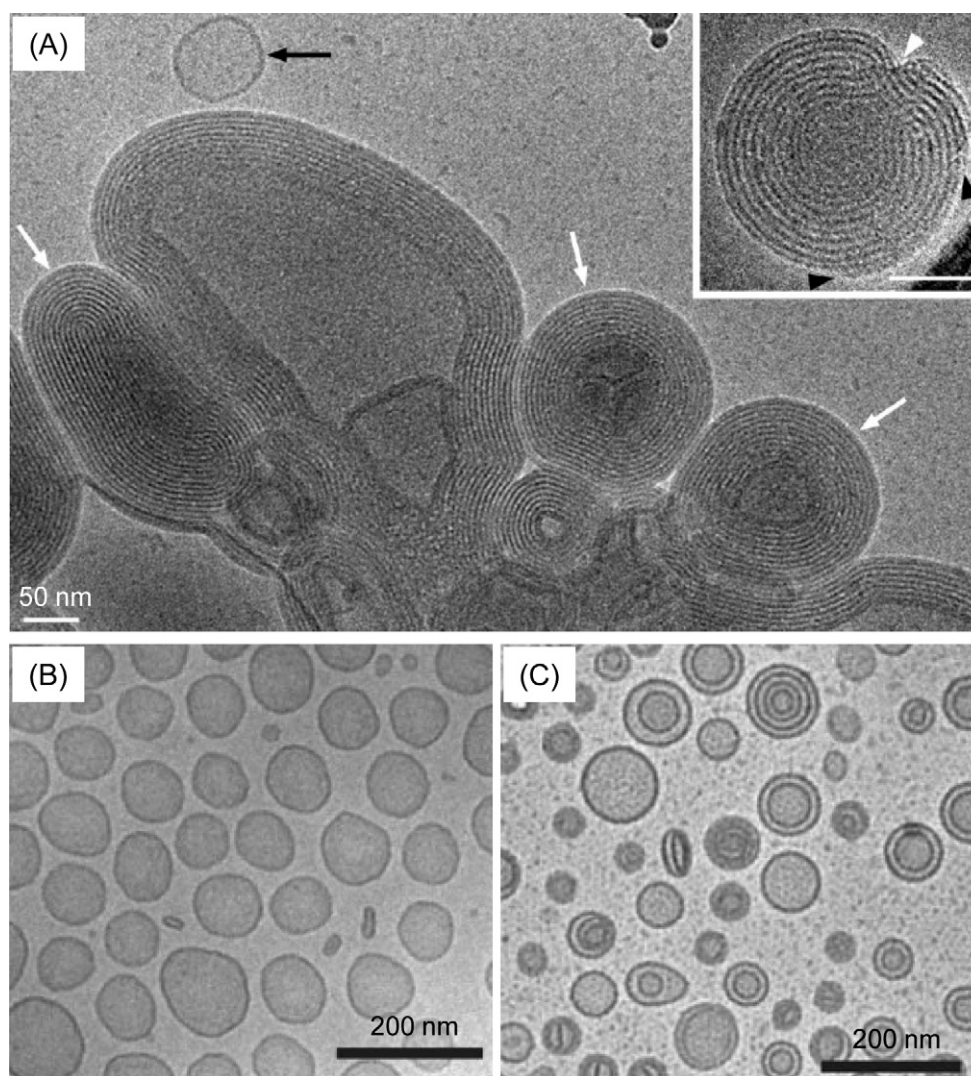


**Fig. 10.** Cryo-TEM image of a lipoplex of N-(1-(2,3-dioleoyloxy)propyl),N,N,N-trimethylammonium chloride (DOTAP) with an oligodeoxynucleotide (ODN) at the isoelectric point (A). Aggregation of condensed multilamellar particles (white arrows), coexisting free liposomes (black arrow). Inset: Lipoplex of DOTAP/cholesterol 1:1 with the ODN (charge ratio 1) at higher magnification; black arrowheads indicate incomplete outer bilayers, the white arrowhead marks a lamellar defect. Cryo-TEM images of stabilized plasmid lipid particles (SPLP) prepared by detergent dialysis (B) or by stepwise ethanol dilution (C). Reprinted from Weisman et al. (2004), with permission from Elsevier (A) and with kind permission from Springer Science and Business Media: Jeffs et al. (2005, Fig. 7a and b) (B and C).

lar structures also form upon interaction of siRNA with cationic lipidic molecules (Desigaux et al., 2007; Geusens et al., 2009). Dispersions with rather small particles (around 100 nm), a reasonably narrow particle size distribution and different morphology were observed upon complexation of siRNA with two cationic lipid:cholesterol:PEG-lipid combinations of different molar ratio (Crawford et al., 2011). Using these two formulations as an example, the usefulness of a sophisticated, semi-automated analysis procedure to obtain comprehensive information on the particle size distribution from cryo-TEM images was demonstrated. It remains, however, to be shown whether this procedure can also be reliably performed on more complex systems.

Most of the aforementioned complexes were rather heterogeneous in size and structure. In order to obtain small particles of more regular structure the so-called stabilized plasmid lipid particles (SPLP) were developed. When prepared by the originally described detergent dialysis procedure with subsequent removal of free DNA and empty liposomes, SPLP consist of a core containing a single plasmid and are surrounded by a lipid membrane (Tam et al., 2000). SPLP formulations manufactured by a modified, more rapid procedure based on the controlled, continuous mixture of the

plasmid solution with an ethanolic solution of the lipids and stepwise dilution were of more heterogeneous structure (Fig. 10B and C) (Jeffs et al., 2005).

In addition to lipids, cationic polymers are also often used to condense DNA. When visualized with cryo-TEM, the resulting polyplexes are frequently of less defined morphology and internal structure than lipoplexes (Agarwal et al., 2007; Ainalem et al., 2009; Sharma et al., 2008). Further processing of polyplexes can result in lipopolyplexes, in which the polyplexes are coated by one or more layers of lipid. For example, Tagawa et al. (2002) obtained very homogenous ternary particles when adding cationic liposomes to negatively charged complexes of plasmid DNA and adenovirus core peptide under optimized preparation conditions. The formation of more heterogeneous particle populations with multilamellar features was observed after incubation of amorphous oligonucleotide/protamine complexes with negatively charged liposomes or mixing of anionic lipid/protamine mixtures with oligonucleotides (Jin et al., 2010; Yang et al., 2009). Association of poly(ethylene imine)/plasmid DNA complexes with a lipid mixture containing anionic as well as PEG-lipids led to the formation of quite homogenous dispersions and the lipid coat on the amor-



phous core of the particles could clearly be visualized (Heyes et al., 2007). For poly(ethylene imine)/oligonucleotide-based lipopolyplexes carrying biotinylated ligands, the ligand affinity could be proven by cryo-TEM using streptavidin conjugated gold nanoparticles (Ko et al., 2009). In addition to lipid-coated polyplexes, the structure of lipid-coated lipopolyplexes and of lipopolyplexes incorporated into emulsions of neutral oil was also studied by cryo TEM (Bartsch et al., 2004, Vonarbourg et al., 2009).

### 3.8. Miscellaneous

Cryo-TEM imaging has also been used for the investigation of nanoparticulate dispersions of pure drugs or drug conjugates. It was, for example, employed to visualize the shape of amorphous and crystalline felodipine nanoparticles prepared by different methods (Lindfors et al., 2007). In phospholipid-containing emulsions of supercooled ubiquinol (coenzyme Q<sub>10</sub>) phospholipid vesicles were observed beside the droplets of the active substance (Siekmann and Westesen, 1995). Couvreur et al. found hexagonally structured, faceted nanoassemblies surrounded by a shell in aqueous dispersions of a gemcitabine squalene conjugate (Couvreur et al., 2008). Spherical particles with an apparently amorphous solid core were found in dispersions formed by ethanol injection of a lipophilic prodrug of paclitaxel in combination with PEGylated phospholipid (Perkins et al., 2000). Complex formation of drugs with oppositely charged surfactants or fatty acid salts in different ratios led to the formation of catanionic vesicles or micelles (Bramer et al., 2006, Dew et al., 2008).

Margulis-Goshen et al. (2010) reported on cryo-TEM investigations on a celecoxib microemulsion prepared with a volatile organic phase that was used to prepare drug-containing nanoassemblies by spray-drying and redispersion in water. The cage-like structure of immune-stimulating complexes (ISCOMS) and their modified derivatives (Posintro<sup>TM</sup> nanoparticles) of 40–50 nm size could be visualized by a Danish group who also investigated the interaction of these colloids with stratum corneum liposomes (Madsen et al., 2010).

Some authors employed cryo-TEM to address questions related to biopharmaceutics. For example, the colloidal structure of simulated intestinal fluids and the processes during lipolytic digestion of drug carrier systems were elucidated by comprehensive cryo-TEM studies (Fatouros et al., 2007, 2009; Kleberg et al., 2010). Szebeni et al. (2001) showed impressive cryo-TEM results on the potential of paclitaxel to precipitate from its micellar solution after dilution of a Cremophor EL/ethanol concentrate with PBS and on the effects of Taxol<sup>®</sup> dilutions on the ultrastructure of human plasma.

## 4. Summary and conclusion

Cryo-TEM has an enormous potential for the structural investigation of colloidal drug delivery systems like liposomes, lipid emulsions and suspensions, lipo- and polyplexes with nucleic acids or nanoparticles based on liquid crystalline phases and to study their interaction with body fluids. For studies on certain delivery systems, e.g. nanoparticles based on lyotropic mesophases, it has developed into an almost indispensable tool. With the increasing availability of the technique and improved possibilities for well-controlled sample preparation its use in the pharmaceutical field is assumed to become more widespread although it will probably remain a method for the clarification of selected basic structural questions rather than for routine quality control issues due to the related costs and comparatively low throughput of samples. Cryo-TEMs with high resolution providing access to advanced techniques like cryo-tomography, will further expand the possibilities to obtain three-dimensional information on the structures of inter-

est. It may be speculated that, under favorable circumstances, they might even allow to investigate the interaction of nanoparticles with cells in more detail in the future.

## Acknowledgement

We would like to thank Frank Steiniger, Friedrich-Schiller-Universität Jena, Germany, for his continuous assistance during our cryo-TEM studies leading to several of the images illustrating this review article.

## References

- Abraham, S.A., Edwards, K., Karlsson, G., Hudon, N., Mayer, L.D., Bally, M.B., 2004. An evaluation of transmembrane ion gradient-mediated encapsulation of topotecan within liposomes. *J. Control. Rel.* 96, 449–461.
- Abraham, S.A., Edwards, K., Karlsson, G., MacIntosh, S., Mayer, L.D., McKenzie, C., Bally, M.B., 2002. Formation of transition metal–doxorubicin complexes inside liposomes. *Biochim. Biophys. Acta* 1565, 41–54.
- Adrian, M., Dubochet, J., Fuller, S.D., Harris, J.R., 1998. Cryo-negative staining. *Micron* 29, 145–160.
- Agarwal, A., Vilensky, R., Stockdale, A., Talmon, Y., Unfer, R.C., Mallapragada, S.K., 2007. Colloidally stable novel copolymeric system for gene delivery in complete growth media. *J. Control. Rel.* 121, 28–37.
- Ainalem, M.L., Carnerup, A.M., Janiak, J., Alfredsson, V., Nylander, T., Schillén, K., 2009. Condensing DNA with poly(amido amine) dendrimers of different generations: means of controlling aggregate morphology. *Soft Matter* 5, 2310–2320.
- Alfredsson, V., 2005. Cryo-TEM studies of DNA and DNA-lipid structures. *Curr. Opin. Colloid Interface Sci.* 10, 269–273.
- Allen, T.M., Cullis, P.R., 2004. Drug delivery systems entering the mainstream. *Science* 303, 1818–1822.
- Almgren, M., Borné, J., Feitosa, E., Khan, A., Lindman, B., 2007. Dispersed lipid liquid crystalline phases stabilized by a hydrophobically modified cellulose. *Langmuir* 23, 2768–2777.
- Almgren, M., Edwards, K., Karlsson, G., 2000. Cryo transmission electron microscopy of liposomes and related structures. *Colloids Surf. A* 174, 3–21.
- Amar-Yuli, I., Wachtel, E., Ben Shoshan, E., Danino, D., Aserin, A., Garti, N., 2007. Hexosome and hexagonal phases mediated by hydration and polymeric stabilizer. *Langmuir* 23, 3637–3645.
- Barauskas, J., Johnsson, M., Jobsson, F., Tiberg, F., 2005a. Cubic phase nanoparticles (Cubosome): principles for controlling size, structure, and stability. *Langmuir* 21, 2569–2577.
- Barauskas, J., Johnsson, M., Tiberg, F., 2005b. Self-assembled lipid superstructures: beyond vesicles and liposomes. *Nano Lett.* 5, 1615–1619.
- Barauskas, J., Misiunas, A., Gunnarsson, T., Tiberg, F., Johnsson, M., 2006. “Sponge” nanoparticle dispersions in aqueous mixtures of diglycerol monooleate, glycerol dioleate, and polysorbate 80. *Langmuir* 22, 6328–6334.
- Bartsch, M., Weeke-Klimp, A.H., Hoenselaar, E.P.D., Stuart, M.C.A., Meijer, D.K.F., Scherphoff, G.L., Kamps, J.A.A.M., 2004. Stabilized lipid coated lipopolyplexes for the delivery of antisense oligonucleotides to liver endothelial cells in vitro and in vivo. *J. Drug Target.* 12, 613–621.
- Belkoura, L., Stubenrauch, C., Strey, R., 2004. Freeze fracture direct imaging: a new freeze fracture method for specimen preparation in cryo-transmission electron microscopy. *Langmuir* 20, 4391–4399.
- Boyd, B.J., Rizwan, S.B., Dong, Y.D., Hook, S., Rades, T., 2007. Self-assembled geometric liquid-crystalline nanoparticles imaged in three dimensions: hexosomes are not necessarily flat hexagonal prisms. *Langmuir* 23, 12461–12464.
- Boyd, B.J., Whittaker, D.V., Khoo, S.M., Davey, G., 2006. Hexosomes formed from glycerate surfactants – formulation as a colloidal carrier for irinotecan. *Int. J. Pharm.* 318, 154–162.
- Bramer, T., Dew, N., Edsman, K., 2006. Catanionic mixtures involving a drug: a rather general concept that can be utilized for prolonged drug release from gels. *J. Pharm. Sci.* 95, 769–780.
- Bunjes, H., Drechsler, M., Koch, M.H.J., Westesen, K., 2001. Incorporation of the model drug ubiquinol into solid lipid nanoparticles. *Pharm. Res.* 18, 287–293.
- Bunjes, H., Koch, M.H.J., Westesen, K., 2000. Effect of particle size on colloidal solid triglycerides. *Langmuir* 16, 5234–5241.
- Bunjes, H., Steiniger, F., Richter, W., 2007. Visualizing the structure of triglyceride nanoparticles in different crystal modifications. *Langmuir* 23, 4005–4011.
- Changsan, N., Chan, H.K., Separovic, F., Srichana, T., 2009. Physicochemical characterization and stability of rifampicin liposome dry powder formulations for inhalation. *J. Pharm. Sci.* 98, 628–639.
- Chiu, G.N.C., Abraham, S.A., Ickenstein, L.M., Ng, R., Karlsson, G., Edwards, K., Wasan, E.K., Bally, M.B., 2005. Encapsulation of doxorubicin into thermosensitive liposomes via complexation with the transition metal manganese. *J. Control. Rel.* 104, 271–288.
- Ciobanu, M., Heurtaut, B., Schultz, P., Ruhlmann, C., Muller, C.D., Frisch, B., 2007. Layersome: development and optimization of stable liposomes as drug delivery system. *Int. J. Pharm.* 344, 154–157.
- Clement, J., Kiefer, K., Kimpfler, A., Garidel, P., Peschka-Süss, R., 2005. Large-scale production of lipopolyplexes with long shelf-life. *Eur. J. Pharm. Biopharm.* 59, 35–43.

- Costello, M.J., 2006. Cryo-electron microscopy of biological samples. *Ultrastruct. Pathol.* 30, 361–371.
- Couvreur, P., Reddy, L.H., Mangenot, S., Poupaert, J.H., Desmaële, D., Lepître-Mouelhi, S., Pili, B., Bourgaux, C., Amenitsch, H., Ollivon, M., 2008. Discovery of new hexagonal supramolecular nanostructures formed by squalenoylation of an anticancer nucleoside analogue. *Small* 4, 247–253.
- Couvreur, P., Vauthier, C., 2006. Nanotechnology: intelligent design to treat complex disease. *Pharm. Res.* 23, 1417–1450.
- Crassous, J.J., Ballauff, M., Drechsler, M., Schmidt, J., Talmon, Y., 2006. Imaging the volume transition in thermosensitive core-shell particles by cryo-transmission electron microscopy. *Langmuir* 22, 2403–2406.
- Crassous, J.J., Rochette, C.N., Wittemann, A., Schrinner, M., Ballauff, M., Drechsler, M., 2009. Quantitative analysis of polymer colloids by cryo-transmission electron microscopy. *Langmuir* 25, 7862–7871.
- Crawford, R., Dogdas, B., Keough, E., Haas, R.M., Wepukhulu, W., Krotzer, S., Burke, P.A., Sepp-Lorenzino, L., Bagchi, A., Howell, B.J., 2011. Analysis of lipid nanoparticles by Cryo-EM for characterizing siRNA delivery vehicles. *Int. J. Pharm.* 403, 237–244.
- de Campo, L., Yagmur, A., Sagalowicz, L., Leser, M.E., Watzke, H., Glatter, O., 2004. Reversible phase transitions in emulsified nanostructured lipid systems. *Langmuir* 20, 5254–5261.
- de Vries, A., Custers, E., Lub, J., van den Bosch, S., Nicolay, K., Grull, H., 2010. Block-copolymer-stabilized iodinated emulsions for use as CT contrast agents. *Biomaterials* 31, 6537–6544.
- del Barrio, J., Oriol, L., Sánchez, C., Serrano, J.L., Di Cicco, A., Keller, P., Li, M.H., 2010. Self-assembly of linear-dendritic diblock copolymers: from nanofibers to polymersomes. *J. Am. Chem. Soc.* 132, 3762–3769.
- Desigaux, L., Sainlos, M., Lambert, O., Chevre, R., Letrou-Bonneval, E., Vigneron, J.P., Lehn, P., Lehn, J.M., Pitard, B., 2007. Self-assembled lamellar complexes of siRNA with lipidic aminoglycoside derivatives promote efficient siRNA delivery and interference. *Proc. Nat. Acad. Sci.* 104, 16534–16539.
- Dew, N., Bramer, T., Edsman, K., 2008. Catanionic aggregates formed from drugs and lauric or capric acids enable prolonged release from gels. *J. Colloid Interface Sci.* 323, 386–394.
- Discher, B.M., Won, Y.Y., Ege, D.S., Lee, J.C.M., Bates, F.S., Discher, D.E., Hammer, D.A., 1999. Polymersomes: tough vesicles made from diblock copolymers. *Science* 284, 1143–1146.
- Dos Santos, N., Mayer, L.D., Abraham, S.A., Gallagher, R.C., Cox, K.A.K., Tardi, P.G., Bally, M.B., 2002. Improved retention of idarubicin after intravenous injection obtained for cholesterol-free liposomes. *Biochim. Biophys. Acta* 1561, 188–201.
- Dragicevic-Curic, N., Scheglmann, D., Albrecht, V., Fahr, A., 2008. Temoporfin-loaded invasomes: development, characterization and in vitro skin penetration studies. *J. Control. Rel.* 127, 59–69.
- Edwards, K., Johnsson, M., Karlsson, G., Silwander, M., 1997. Effect of polyethyleneglycol-phospholipids on aggregate structure in preparations of small unilamellar liposomes. *Biophys. J.* 73, 258–266.
- Efrat, R., Kesselman, E., Aserin, A., Garti, N., Danino, D., 2009. Solubilization of hydrophobic guest molecules in the monoolein discontinuous  $Q_1$  cubic mesophase and its soft nanoparticles. *Langmuir* 25, 1316–1326.
- Egelhaaf, S.U., Schurtenberger, P., Müller, M., 2000. New controlled environment vitrification system for cryo-transmission electron microscopy: design and application to surfactant solutions. *J. Microsc.* 200, 128–139.
- Esposito, E., Cortesi, R., Drechsler, M., Paccamiccio, L., Mariani, P., Contado, C., Stellin, E., Menegatti, E., Bonina, F., Puglia, C., 2005. Cubosome dispersions as delivery systems for percutaneous administration of indomethacin. *Pharm. Res.* 22, 2163–2173.
- Esposito, E., Fantin, M., Marti, M., Drechsler, M., Paccamiccio, L., Mariani, P., Sivieri, E., Lain, F., Menegatti, E., Morari, M., Cortesi, R., 2008. Solid lipid nanoparticles as delivery systems for bromocriptine. *Pharm. Res.* 25, 1521–1530.
- Fatouros, D.G., Bergenstahl, B., Müllertz, A., 2007. Morphological observations on a lipid-based drug delivery system during in vitro digestion. *Eur. J. Pharm. Sci.* 31, 85–94.
- Fatouros, D.G., Walrand, I., Bergenstahl, B., Müllertz, A., 2009. Colloidal structures in media simulating intestinal fed state conditions with and without lipolysis products. *Pharm. Res.* 26, 361–374.
- Firestone, R.A., 1994. Low-density lipoprotein as a vehicle for targeting antitumor compounds to cancer cells. *Bioconj. Chem.* 5, 105–113.
- Fondell, A., Edwards, K., Ickenstein, L.M., Sjöberg, S., Carlsson, J., Gedda, L., 2010. Nuclisome: a novel concept for radionuclide therapy using targeting liposomes. *Eur. J. Nucl. Med. Mol. Imaging* 37, 114–123.
- Frederik, P.M., Hubert, D.H., 2005. Cryoelectron microscopy of liposomes. *Methods Enzymol.* 391, 431–448.
- Friedrich, H., Frederik, P.M., de With, G., Sommerdijk, N.A.J.M., 2010. Imaging of self-assembled structures: interpretation of TEM and cryo-TEM images. *Angew. Chem. Int. Ed.* 49, 7850–7858.
- Fritze, A., Hens, F., Kimpfler, A., Schubert, R., Peschka-Stüss, R., 2006. Remote loading of doxorubicin into liposomes driven by a transmembrane phosphate gradient. *Biochim. Biophys. Acta* 1758, 1633–1640.
- Gan, L., Han, S., Shen, J., Zhu, J., Zhu, C., Zhang, X., Gan, Y., 2010. Self-assembled liquid crystalline nanoparticles as a novel ophthalmic delivery system for dexamethasone: improving preocular retention and ocular bioavailability. *Int. J. Pharm.* 396, 179–187.
- Geusens, B., Lambert, J., De Smedt, S.C., Buyens, K., Sanders, N.N., Van Gele, M., 2009. Ultradefinable cationic liposomes for delivery of small interfering RNA (siRNA) into human primary melanocytes. *J. Control. Rel.* 133, 214–220.
- Ghoroghchian, P.P., Lin, J.J., Brannan, A.K., Frail, P.R., Bates, F.S., Therien, M.J., Hammer, D.A., 2006. Quantitative membrane loading of polymer vesicles. *Soft Matter* 2, 973–980.
- Grassucci, R.A., Taylor, D., Frank, J., 2007. Preparation of macromolecular complexes for cryo-electron microscopy. *Nat. Protoc.* 2, 3239–3246.
- Grassucci, R.A., Taylor, D., Frank, J., 2008. Visualization of macromolecular complexes using cryo-electron microscopy with FEI Tecnai transmission electron microscopes. *Nat. Protoc.* 3, 330–339.
- Gustafsson, J., Arvidson, G., Karlsson, G., Almgren, M., 1995. Complexes between cationic liposomes and DNA visualized by cryo-TEM. *Biochim. Biophys. Acta* 1235, 305–312.
- Gustafsson, J., Ljusberg-Wahren, H., Almgren, M., Larsson, K., 1997. Submicron particles of reversed lipid phases in water stabilized by a nonionic amphiphilic polymer. *Langmuir* 13, 6964–6971.
- Hans, M., Shimoni, K., Danino, D., Siegel, S.J., Lowman, A., 2005. Synthesis and characterization of mPEG-PLA prodrug micelles. *Biomacromolecules* 6, 2708–2717.
- Harris, J.R., 1997. Negative Staining and Cryoelectron Microscopy. Bios Scientific Publishers, Oxford, UK.
- Harris, J.R., 2007. Negative staining of thinly spread biological samples. In: Kuo, J. (Ed.), *Electron Microscopy: Methods and Protocols*, second ed. Humana Press, Totowa, NJ, pp. 107–142, *Methods Mol. Biol.* 369.
- Heyes, J., Palmer, L., Chan, K., Giesbrecht, C., Jeffs, L., MacLachlan, I., 2007. Lipid encapsulation enables the effective systemic delivery of polyplex plasmid DNA. *Mol. Ther.* 15, 713–720.
- Holzer, M., Barnert, S., Momm, J., Schubert, R., 2009. Preparative size exclusion chromatography combined with detergent removal as a versatile tool to prepare unilamellar and spherical liposomes of highly uniform size distribution. *J. Chromatogr. A* 1216, 5838–5848.
- Huebner, S., Battersby, B.J., Grimm, R., Cevc, G., 1999. Lipid-DNA complex formation: reorganization and rupture of lipid vesicles in the presence of DNA as observed by cryoelectron microscopy. *Biophys. J.* 76, 3158–3166.
- Ickenstein, L.M., Sandström, M.C., Mayer, L.D., Edwards, K., 2006. Effects of phospholipid hydrolysis on the aggregate structure in DPPC/DSPE-PEG2000 liposome preparations after gel to liquid crystalline phase transition. *Biochim. Biophys. Acta* 1758, 171–180.
- Jeffs, L.B., Palmer, L.R., Ambegia, E.G., Giesbrecht, C., Ewanick, S., MacLachlan, I., 2005. A scalable, extrusion-free method for efficient liposomal encapsulation of plasmid DNA. *Pharm. Res.* 22, 362–372.
- Jiang, W., Chiu, W., 2007. Cryoelectron microscopy of icosahedral virus particles. In: Kuo, J. (Ed.), *Electron Microscopy: Methods and Protocols*, second ed. Humana Press, Totowa, NJ, pp. 345–363, *Methods Mol. Biol.* 369.
- Jin, Y., Liu, S., Yu, B., Golan, S., Koh, C.G., Yang, J., Huynh, L., Yang, X., Pang, J., Muthusamy, N., Chan, K.K., Byrd, J.C., Talmon, Y., Lee, L.J., Lee, R.J., Marcucci, G., 2010. Targeted delivery of antisense oligodeoxynucleotide by transferrin conjugated pH-sensitive lipopolyplex nanoparticles: a novel oligonucleotide-based therapeutic strategy in acute myeloid leukemia. *Mol. Pharm.* 7, 196–206.
- Johnsson, M., Barauskas, J., Norlin, A., Tiberg, F., 2006. Physicochemical and drug delivery aspects of lipid-based liquid crystalline nanoparticles: a case study of intravenously administered propofol. *J. Nanosci. Nanotechnol.* 6, 3017–3024.
- Johnsson, M., Barauskas, J., Tiberg, F., 2005a. Cubic phases and cubic phase dispersions in a phospholipid-based system. *J. Am. Chem. Soc.* 127, 1076–1077.
- Johnsson, M., Edwards, K., 2001. Phase behavior and aggregate structure in mixtures of dioleoylphosphatidylethanolamine and poly(ethylene glycol)-lipids. *Biophys. J.* 80, 313–323.
- Johnsson, M., Edwards, K., 2003. Liposomes, disks, and spherical micelles: aggregate structure in mixtures of gel phase phosphatidylcholines and poly(ethylene glycol)-phospholipids. *Biophys. J.* 85, 3839–3847.
- Johnsson, M., Lam, Y., Barauskas, J., Tiberg, F., 2005b. Aqueous phase behavior and dispersed nanoparticles of diglycerol monooleate/glycerol dioleate mixtures. *Langmuir* 21, 5159–5165.
- Johnston, M.J.W., Semple, S.C., Klimuk, S.K., Edwards, K., Eisenhardt, M.L., Leng, E.C., Karlsson, G., Yanko, D., Cullis, P.R., 2006. Therapeutically optimized rates of drug release can be achieved by varying the drug-to-lipid ratio in liposomal vincristine formulations. *Biochim. Biophys. Acta* 1758, 55–64.
- Jores, K., Mehnert, W., Drechsler, M., Bunjes, H., Johann, C., Mäder, K., 2004. Investigations on the structure of solid lipid nanoparticles (SLN) and oil-loaded solid lipid nanoparticles by photon correlation spectroscopy, field-flow fractionation and transmission electron microscopy. *J. Control. Rel.* 95, 217–227.
- Kaiser, N., Kimpfler, A., Massing, U., Burger, A.M., Fiebig, H.H., Brandl, M., Schubert, R., 2003. 5-Fluorouracil in vesicular phospholipid gels for anticancer treatment: entrapment and release properties. *Int. J. Pharm.* 256, 123–131.
- Kim, S.H., Haimovich-Caspi, L., Omer, L., Talmon, Y., Franses, E.I., 2007. Effect of sonication and freezing-thawing on the aggregate size and dynamic surface tension of aqueous DPPC dispersions. *J. Colloid Interface Sci.* 311, 217–227.
- Kim, S.Y., Lee, K.E., Han, S.S., Jeong, B., 2008. Vesicle-to-spherical micelle-to tubular nanostructure transition of monomethoxy-poly(ethylene glycol)-poly(trimethylene carbonate) diblock copolymer. *J. Phys. Chem. B* 112, 7420–7423.
- Klang, V., Matsko, N., Zimmermann, A.M., Vojnikovic, E., Valenta, C., 2010. Enhancement of stability and skin permeation by sucrose stearate and cyclodextrins in progesterone nanoemulsions. *Int. J. Pharm.* 393, 152–160.
- Kleberg, K., Jacobsen, F., Fatouros, D.G., Müllertz, A., 2010. Biorelevant media simulating fed state intestinal fluids: colloid phase characterization and impact on solubilization capacity. *J. Pharm. Sci.* 99, 3522–3532.
- Ko, Y.T., Bhattacharya, R., Bickel, U., 2009. Liposome encapsulated polyethyleneimine/ODN polyplexes for brain targeting. *J. Control. Rel.* 133, 230–237.

- Koning, R.I., Koster, A.J., 2009. Cryo-electron tomography in biology and medicine. *Ann. Anat.* 191, 427–445.
- Kuntsche, J., Freisleben, I., Steiniger, F., Fahr, A., 2010a. Temoporfin-loaded liposomes: physicochemical characterization. *Eur. J. Pharm. Sci.* 40, 305–315.
- Kuntsche, J., Klaus, K., Steiniger, F., 2009. Size determinations of colloidal fat emulsions: a comparative study. *J. Biomed. Nanotechnol.* 5, 384–395.
- Kuntsche, J., Koch, M.H.J., Drechsler, M., Bunjes, H., 2005. Crystallization behavior of supercooled smectic cholesteryl myristate nanoparticles containing phospholipids as stabilizers. *Colloids Surf. B* 44, 25–35.
- Kuntsche, J., Koch, M.H.J., Steiniger, F., Bunjes, H., 2010b. Influence of stabilizer systems on the properties and phase behavior of supercooled smectic nanoparticles. *J. Colloid Interface Sci.* 350, 229–239.
- Kuntsche, J., Westesen, K., Drechsler, M., Koch, M.H.J., Bunjes, H., 2004. Supercooled smectic nanoparticles: a potential novel carrier system for poorly water soluble drugs. *Pharm. Res.* 21, 1834–1843.
- Li, X., Hirsh, D.J., Cabral-Lilly, D., Zirkel, A., Gruner, S.M., Janoff, A.S., Perkins, W.R., 1998. Doxorubicin physical state in solution and inside liposomes loaded via a pH gradient. *Biochim. Biophys. Acta* 1415, 23–40.
- Lindfors, L., Skantze, P., Skantze, U., Westergren, J., Olsson, U., 2007. Amorphous drug nanosuspensions. 3. Particle dissolution and crystal growth. *Langmuir* 23, 9866–9874.
- Madsen, H.B., Arboe-Andersen, H.M., Rozlosnik, N., Madsen, F., Iversen, P., Kasimova, M.R., Nielsen, H.M., 2010. Investigation of the interaction between modified ISCOMs and stratum corneum lipid model systems. *Biochim. Biophys. Acta* 1798, 1779–1789.
- Margulis-Goshen, K., Kesselman, E., Danino, D., Magdassi, S., 2010. Formation of celecoxib nanoparticles from volatile microemulsions. *Int. J. Pharm.* 393, 230–237.
- Marko, M., Hsieh, C.E., 2007. Three-dimensional cryotransmission electron microscopy of cells and organelles. In: Kuo, J. (Ed.), *Electron Microscopy: Methods and Protocols*, second ed. Humana Press, Totowa, NJ, pp. 407–429, *Methods Mol. Biol.* 369.
- Maurer, N., Wong, K.F., Stark, H., Louie, L., McIntosh, D., Wong, T., Scherrer, P., Semple, S.C., Cullis, P.R., 2001. Spontaneous entrapment of polynucleotides upon electrostatic interaction with ethanol-destabilized cationic liposomes. *Biophys. J.* 80, 2310–2326.
- Milne, J.L.S., Subramaniam, S., 2009. Cryo-electron tomography of bacteria: progress, challenges and future prospects. *Nat. Rev. Microbiol.* 7, 666–675.
- Murgia, S., Falchi, A.M., Mano, M., Lampis, S., Angius, R., Carnerup, A.M., Schmidt, J., Diaz, G., Giacca, M., Talmon, Y., Monduzzi, M., 2010. Nanoparticles from lipid-based liquid crystals: emulsifier influence on morphology and cytotoxicity. *J. Phys. Chem. B* 114, 3518–3525.
- Norlén, L., 2007. Nanostructure of the stratum corneum extracellular lipid matrix as observed by cryo-electron microscopy of vitreous skin sections. *Int. J. Cosm. Sci.* 29, 335–352.
- Orlova, E.V., Sherman, M.B., Chiu, W., Mowri, H., Smith, L.C., Gotto, A.M., 1999. Three-dimensional structure of low density lipoproteins by electron cryomicroscopy. *Proc. Natl. Acad. Sci.* 96, 8420–8425.
- Perkins, W.R., Ahmad, I., Li, X., Hirsh, D.J., Masters, G.R., Fecko, C.J., Lee, J.K., Ali, S., Nguyen, J., Schupsky, J., Herbert, C., Janoff, A.S., Mayhew, E., 2000. Novel therapeutic nano-particles (lipocores): trapping poorly water soluble compounds. *Int. J. Pharm.* 200, 27–39.
- Perrie, Y., Frederik, P.M., Gregoriadis, G., 2001. Liposome-mediated DNA vaccination: the effect of vesicle composition. *Vaccine* 19, 3301–3310.
- Petersen, S., Steiniger, F., Fischer, D., Fahr, A., Bunjes, H. The physical state of lipid nanoparticles influences their effect on in vitro cell viability. Submitted for publication.
- Petrov, P.D., Drechsler, M., Müller, A.H.E., 2009. Self-assembly of asymmetric poly(ethylene oxide)-block-poly(n-butyl acrylate) diblock copolymers in aqueous media to unexpected morphologies. *J. Phys. Chem. B* 113, 4218–4225.
- Rangelov, S., Almgren, M., 2005. Particulate and bulk bicontinuous cubic phases obtained from mixtures of glyceryl monooleate and copolymers bearing blocks of lipid-mimetic anchors in water. *J. Phys. Chem. B* 109, 3921–3929.
- Rank, A., Hauschild, S., Förster, S., Schubert, R., 2009. Preparation of monodisperse block copolymer vesicles via a thermotropic cylinder-vesicle transition. *Langmuir* 25, 1337–1344.
- Rodríguez-Pulido, A., Ortega, F., Llorca, O., Aicart, E., Junquera, E., 2008. A physicochemical characterization of the interaction between DC-Chol/DOPE cationic liposomes and DNA. *J. Phys. Chem. B* 112, 12555–12565.
- Roos, N., Morgan, A.J., 1990. *Imaging and Analysis of Frozen-Hydrated Specimens, Cryopreparation of Thin Biological Specimen for Electron Microscopy: Methods and Applications*. Oxford University Press, Oxford.
- Rosenblatt, K.M., Bunjes, H., 2009. Poly(vinyl alcohol) as emulsifier stabilizes solid triglyceride drug carrier nanoparticles in the  $\alpha$ -modification. *Mol. Pharm.* 6, 105–120.
- Rotenberg, M., Rubin, M., Bor, A., Meyuh, D., Talmon, Y., Lichtenberg, D., 1991. Physico-chemical characterization of Intralipid™ emulsions. *Biochim. Biophys. Acta* 1086, 265–272.
- Sagalowicz, L., Acquistapace, S., Watzke, H.J., Michel, M., 2007. Study of liquid crystal space groups using controlled tilting with cryogenic transmission electron microscopy. *Langmuir* 23, 12003–12009.
- Sagalowicz, L., Michel, M., Adrian, M., Frossard, P., Rouvet, M., Watzke, H.J., Yaghmur, A., de Campo, L., Glatter, O., Liser, M.E., 2006. Crystallography of dispersed liquid crystalline phases studied by cryo-transmission electron microscopy. *J. Microsc.* 221, 110–121.
- Sandström, M.C., Johansson, E., Edwards, K., 2008. Influence of preparation path on the formation of discs and threadlike micelles in DSPE-PEG2000/lipid systems. *Biophys. Chem.* 132, 97–103.
- Semple, S.C., Klimuk, S.K., Harasym, T.O., Dos Santos, N., Ansell, S.M., Wong, K.F., Maurer, N., Stark, H., Cullis, P.R., Hope, M.J., Scherrer, P., 2001. Efficient encapsulation of antisense oligonucleotides in lipid vesicles using ionizable aminolipids: formation of novel small multilamellar vesicle structures. *Biochim. Biophys. Acta* 1510, 152–166.
- Semple, S.C., Leone, R., Wang, J., Leng, E.C., Klimuk, S.K., Eisenhardt, M.L., Yuan, Z.N., Edwards, K., Maurer, N., Hope, M.J., Cullis, P.R., Ahkong, Q.F., 2005. Optimization and characterization of a sphingomyelin/cholesterol liposome formulation of vinorelbine with promising antitumor activity. *J. Pharm. Sci.* 94, 1024–1038.
- Severs, N.J., 2007. Freeze-fracture electron microscopy. *Nat. Protoc.* 2, 547–576.
- Sharma, R., Lee, J.S., Bettencourt, R.C., Xiao, C., Konieczny, S.F., Won, Y.Y., 2008. Effects of the incorporation of a hydrophobic middle block into a PEG-polycation diblock copolymer on the physicochemical and cell interaction properties of the polymer-DNA complexes. *Biomacromolecules* 9, 3294–3307.
- Siekmann, B., Westesen, K., 1995. Preparation and physicochemical characterization of aqueous dispersions of coenzyme Q<sub>10</sub> nanoparticles. *Pharm. Res.* 12, 201–208.
- Sjöström, B., Kaplun, A., Talmon, Y., Cabane, B., 1995. Structures of nanoparticles prepared from oil-in-water emulsions. *Pharm. Res.* 12, 39–48.
- Soga, O., van Nostrum, C.F., Fens, M., Rijken, C.J.F., Schifflers, R.M., Storm, G., Hennink, E.W., 2005. Thermosensitive and biodegradable polymeric micelles for paclitaxel delivery. *J. Control. Rel.* 103, 341–353.
- Song, L., Li, H., Sunar, U., Chen, J., Corbin, I., Yodh, A.G., Zheng, G., 2007. Naphthalocyanine-reconstituted LDL nanoparticles for in vivo cancer imaging and treatment. *Int. J. Nanomed.* 2, 767–774.
- Spicer, P.T., Hayden, K.L., Lynch, M.L., Ofori-Boateng, A., Burns, J.L., 2001. Novel process for producing cubic liquid crystalline nanoparticles (Cubosomes). *Langmuir* 17, 5748–5756.
- Spin, J.M., Atkinson, D., 1995. Cryoelectron microscopy of low density lipoprotein in vitreous ice. *Biophys. J.* 68, 2115–2123.
- Szebeni, J., Alving, C.R., Savay, S., Barenholz, Y., Prieve, A., Danino, D., Talmon, Y., 2001. Formation of complement-activating particles in aqueous solutions of Taxol: possible role in hypersensitivity reactions. *Int. Immunopharmacol.* 1, 721–735.
- Tagawa, T., Manvell, M., Brown, N., Keller, M., Perouzel, E., Murray, K.D., Harbottle, R.P., Teclé, M., Booy, F., Brahimi-Horn, M.C., Coutelle, C., Lemoine, N.R., Alton, E.W., Miller, A.D., 2002. Characterisation of LMD virus-like nanoparticles self-assembled from cationic liposomes, adenovirus core peptide  $\mu$  (mu) and plasmid DNA. *Gene Ther.* 9, 564–576.
- Taggar, A.S., Alnajim, J., Anantha, M., Thomas, A., Webb, M., Ramsay, E., Bally, M.B., 2006. Copper-topotecan complexation mediates drug accumulation into liposomes. *J. Control. Rel.* 114, 78–88.
- Tam, P., Monck, M., Lee, D., Ludkovski, O., Leng, E.C., Clow, K., Stark, H., Scherrer, P., Graham, R.W., Cullis, P.R., 2000. Stabilized plasmid lipid particles for systemic gene therapy. *Gene Ther.* 7, 1867–1874.
- Teixeira, H., Dubernet, C., Rosilio, V., Benita, S., Lepault, J., Erk, I., Couvreur, P., 2000. New bicompartmental structures are observed when stearylamine is mixed with triglyceride emulsions. *Pharm. Res.* 17, 1329–1332.
- Thierry, A.R., Norris, V., Molina, F., Schmutz, M., 2009. Lipoplex nanostructures reveal a general self-organization of nucleic acids. *Biochim. Biophys. Acta* 1790, 385–394.
- Unger, V.M., 2001. Electron cryomicroscopy methods. *Curr. Opin. Struct. Biol.* 11, 548–554.
- Unruh, T., Bunjes, H., Westesen, K., Koch, M.H.J., 1999. Observation of size-dependent melting in lipid nanoparticles. *J. Phys. Chem. B* 103, 10373–10377.
- van Antwerpen, R., Chen, G.C., Pullinger, C.R., Kane, J.P., LaBelle, M., Krauss, R.M., Luna-Chavez, C., Forte, T.M., Gilkey, J.C., 1997. Cryo-electron microscopy of low density lipoprotein and reconstituted discoidal high density lipoprotein: imaging of the apolipoprotein moiety. *J. Lipid Res.* 38, 659–669.
- van Antwerpen, R., Gilkey, J.C., 1994. Cryo-electron microscopy reveals human low density lipoprotein substructure. *J. Lipid Res.* 35, 2223–2231.
- van Antwerpen, R., La Belle, M., Navratilova, E., Krauss, R.M., 1999. Structural heterogeneity of apoB-containing serum lipoproteins visualized using cryo-electron microscopy. *J. Lipid Res.* 40, 1827–1836.
- Vanhecke, D., Studer, L., Studer, D., 2007. *Cryoultramicrotomy*. In: Kuo, J. (Ed.), *Electron Microscopy: Methods and Protocols*, second ed. Humana Press, Totowa, NJ, pp. 175–197, *Methods Mol. Biol.* 369.
- Velluto, D., Dermurats, D., Hubbell, J.A., 2008. PEG-b-PPS diblock copolymer aggregates for hydrophobic drug solubilization and release: cyclosporin A as an example. *Mol. Pharm.* 5, 632–642.
- Vonarbourg, A., Passirani, C., Desigaux, L., Allard, E., Saulnier, P., Lambert, O., Benoit, J.P., Pitard, B., 2009. The encapsulation of DNA molecules within biomimetic lipid nanocapsules. *Biomaterials* 30, 3197–3204.
- Weisman, S., Hirsch-Lerner, D., Barenholz, Y., Talmon, Y., 2004. Nanostructure of cationic lipid-oligonucleotide complexes. *Biophys. J.* 87, 609–614.
- Wessman, P., Edwards, K., Mahlin, D., 2010. Structural effects caused by spray- and freeze-drying of liposomes and bilayer discs. *J. Pharm. Sci.* 99, 2032–2048.
- Westesen, K., Drechsler, M., Bunjes, H., 2001. Colloidal dispersions based on solid lipids. In: Dickinson, E., Miller, R. (Eds.), *Food Colloids: Fundamentals of Formulation*. Royal Society of Chemistry, Cambridge, pp. 103–115.
- Westesen, K., Siekmann, B., 1997. Investigation of the gel formation of phospholipid-stabilized solid lipid nanoparticles. *Int. J. Pharm.* 151, 35–45.
- Wheeler, J.J., Wong, K.F., Ansell, S.M., Masin, D., Bally, M.B., 1994. Polyethylene glycol modified phospholipids stabilize emulsions prepared from triacylglycerol. *J. Pharm. Sci.* 83, 1558–1564.



- Williams, D.B., Carter, C.B., 1996. *Transmission Electron Microscopy. A Textbook for Materials Science. I. Basics*. Springer, New York.
- Witte mann, A., Drechsler, M., Talmon, Y., Ballauff, M., 2005. High elongation of polyelectrolyte chains in the osmotic limit of spherical polyelectrolyte brushes: a study by cryogenic transmission electron microscopy. *J. Am. Chem. Soc.* 127, 9688–9689.
- Wörle, G., Drechsler, M., Koch, M.H.J., Siekmann, B., Westesen, K., Bunjes, H., 2007. Influence of composition and preparation parameters on the properties of aqueous monoolein dispersions. *Int. J. Pharm.* 329, 150–157.
- Wörle, G., Siekmann, B., Koch, M.H.J., Bunjes, H., 2006. Transformation of vesicular into cubic nanoparticles by autoclaving of aqueous monoolein/poloxamer dispersions. *Eur. J. Pharm. Sci.* 27, 44–53.
- Yaghmur, A., de Campo, L., Sagalowicz, L., Leser, M.E., Glatter, O., 2005. Emulsified microemulsions and oil-containing liquid crystalline phases. *Langmuir* 21, 569–577.
- Yaghmur, A., de Campo, L., Salentinig, S., Sagalowicz, L., Leser, M.E., Glatter, O., 2006. Oil-loaded monolinolein-based particles with confined inverse discontinuous cubic structure (Fd3m). *Langmuir* 22, 517–521.
- Yang, J., Pinol, R., Gubellini, F., Lévy, D., Albouy, P.A., Keller, P., Li, M.H., 2006. Formation of polymer vesicles by liquid crystal amphiphilic block copolymers. *Langmuir* 22, 7907–7911.
- Yang, X., Koh, C.G., Liu, S., Pan, X., Santhanam, R., Yu, B., Peng, Y., Pang, J., Golan, S., Talmon, Y., Jin, Y., Muthusamy, N., Byrd, J.C., Chan, K.K., Lee, L.J., Marcucci, G., Lee, R.J., 2009. Transferrin receptor-targeted lipid nanoparticles for delivery of an antisense oligodeoxyribonucleotide against Bcl-2. *Mol. Pharm.* 6, 221–230.
- Yu, S., Azzam, T., Rouiller, I., Eisenberg, A., 2009. “Breathing” vesicles. *J. Am. Chem. Soc.* 131, 10557–10566.
- Zasadzinski, J.A.N., 1986. Transmission electron microscopy observations of sonication-induced changes in liposome structure. *Biophys. J.* 49, 1119–1130.
- Zhigaltsev, I.V., Maurer, N., Edwards, K., Karlsson, G., Cullis, P.R., 2006. Formation of drug-arylsulfonate complexes inside liposomes: a novel approach to improve drug retention. *J. Control. Rel.* 110, 378–386.